



저작자표시-변경금지 2.0 대한민국

이용자는 아래의 조건을 따르는 경우에 한하여 자유롭게

- 이 저작물을 복제, 배포, 전송, 전시, 공연 및 방송할 수 있습니다.
- 이 저작물을 영리 목적으로 이용할 수 있습니다.

다음과 같은 조건을 따라야 합니다:



저작자표시. 귀하는 원저작자를 표시하여야 합니다.



변경금지. 귀하는 이 저작물을 개작, 변형 또는 가공할 수 없습니다.

- 귀하는, 이 저작물의 재이용이나 배포의 경우, 이 저작물에 적용된 이용허락조건을 명확하게 나타내어야 합니다.
- 저작권자로부터 별도의 허가를 받으면 이러한 조건들은 적용되지 않습니다.

저작권법에 따른 이용자의 권리는 위의 내용에 의하여 영향을 받지 않습니다.

이것은 [이용허락규약\(Legal Code\)](#)을 이해하기 쉽게 요약한 것입니다.

[Disclaimer](#)

공학석사 학위논문

Evaluation of Floor Acceleration
Demands for Seismic Design of
Non-structural Components

비구조요소의 내진설계를 위한
등가정적 및 동적 응답 분석

2019년 8월

서울대학교 대학원

건축학과

이 승 호

Evaluation of Floor Acceleration
Demands for Seismic Design of
Non-structural Components

지도교수 이 철 호

이 논문을 공학석사 학위논문으로 제출함

2019년 8월


서울대학교 대학원


건축학과


이 승 호

이승호의 석사 학위논문을 인준함

2019년 8월

위 원 장 홍 성 경 

부위원장 이 철 호 

위 원 박 흥 준 

Abstract

Evaluation of Floor Acceleration Demands for Seismic Design of Non-structural Components

Lee, Seung Ho

Department of Architecture and Architectural Engineering

The Graduate School

Seoul National University

In this study, the commonly used method, equivalent static approach for seismic design of non-structural elements, was evaluated to find the possibility of developing current provisions. To evaluate current design code, ASCE7 is reviewed. By evaluating static load approach suggested in current code provisions, it seemingly revealed shortcomings of the static method while using dynamic method considering fundamental period of supporting structure. A total of five three-dimensional models were analyzed using structural analysis program. In the first set of analysis, 3-, 9-, 20-story three-dimensional SAC building models were evaluated and in the second set of

analysis, 4-, 8-story asymmetrical telecommunication buildings were proposed for analyzing floor spectrum based on linear static analysis and dynamic analysis from ASCE7-16. Dynamic Analysis includes response spectrum analysis, linear time history analysis, nonlinear time history analysis and alternative floor response spectra. The result from both linear static analysis and dynamic analysis is typically used for floor response spectrum for nonstructural elements because each floor's maximum acceleration can mitigate the process of reinforcement for nonstructural elements under earthquakes. Typically, most evaluations for spectrum analysis depend heavily on simplified two-dimensional numerical models.

In this study, the equivalent static method was evaluated based on elementary structural dynamics and numerical case study of realistic three-dimensional model. The inaccuracy of the equivalent static approach resulting from the negligence of the fundamental period of supporting structures was clearly illustrated using elementary structural dynamics. The numerical dynamic analysis of 3-dimensional building models also showed that the magnitude and distribution of the maximum floor acceleration can significantly be influenced by the supporting structural characteristics such as fundamental period, higher modes, nonlinearity and torsion. The current equivalent static approach needs to be improved such that some of the key influential structural parameters are selectively included within the limit of practicality.

**Keywords: Non-structural Elements, Floor acceleration,
Equivalent Static Load, Torsion, Higher mode effect,
Nonlinearity**

Student Number: 2017-28610

Table of Contents

Abstract	i
Table of Contents	iv
List of Figures	vi
Chapter 1 Introduction	9
1.1. Research background.....	9
1.2. Objectives and scope	10
1.3. Outline of thesis.....	13
Chapter 2 Review of Equivalent Static Approach in Design Standards and Previous Studies	14
2.1. Backgrounds of current design standards	14
2.1.1. 1994 NEHRP.....	14
2.1.2. 1994 /1997 UBC.....	15
2.2. Current design codes	17
2.2.1. ASCE7-16.....	17
2.2.1.1. Equivalent static analysis	17
2.2.1.2. Dynamic analysis	18
2.2.2. EUROCODE 8	24
2.3. Previous studies	25
2.3.1. Kehoe and Freeman (1998).....	26
2.3.2. Drake and Bachman (1995).....	27
2.3.3. Singh (1987).....	28
2.3.4. Anajafi and Medina (2018).....	29
2.3.5. Villaverde (2000).....	30
Chapter 3 Evaluation Based on Elementary Dynamic	

Theory	34
3.1. Introduction	34
3.2. Preliminary analysis of instrumented building database	34
3.3. Absolute floor acceleration based on structural dynamics	37
3.4. Response of non-structural element supporting structure's natural frequency	41
3.5. Summary.....	43
Chapter 4 Evaluation of Equivalent Static Method based on Numerical Analysis	44
4.1. Introduction	44
4.2. Numerical model: 3-, 9-, 20-story SAC model, 4-, 8-story telecommunication building model	45
4.3. Effect of structural period.....	46
4.4. Effect of higher modes	47
4.5. Effect of Nonlinearity	52
4.6. Torsion 52	
4.6.1. Introduction	52
4.6.2. Evaluation of ASCE 7-16 method	53
4.7. Floor response spectrum method application	57
Chapter 5 Case study: Effect of a_p, and R_p application	67
5.1. Acceleration sensitive non-structural component.....	67
5.2. Deformation sensitive non-structural component	71
Chapter 6 Summary and Conclusions	75
Bibliography	78
Abstract (in Korean)	81
Acknowledgements	83

List of Figures

Figure 1-1 Non-structural damage due to Korean Earthquake (Lee et al, 2019)	10
Figure 1-2. Flow chart for designing non-structural component (ASCE 7)....	11
Figure 2-1 Torsional Amplification Factor A_x	19
Figure 2-2. Amplification factor for symmetric rectangular buildings	20
Figure 2-3 Component Dynamic Amplification Factor (D_{AF}).....	23
Figure 2-4 Comparison between 1994/ 1997 UBC, (Kehoe and Freeman, 1998)	26
Figure 2-5 Instrumented building data (Drake and Bachman, 1995).....	27
Figure 2-6 Floor response spectra corresponding different mass ratio (Singh, 1987)	28
Figure 2-7. 5% damped normalize roof spectra, (Anajafi and Medina, 2018)	29
Figure 2-8. Assumed mode shapes for components with (a) one and (b) two points of attachment (Villaverde, 2000).....	31
Figure 3-1. Peak floor accelerations as affected by PGA magnitude and building period	35
Figure 3-2 Summary of floor acceleration prediction based on elementary structural dynamics	37
Figure 3-3 Response spectrum used to evaluate theoretical value of floor acceleration	41
Figure 4-1 Three SAC building models designed according to UBC 1994 ...	45
Figure 4-2 4-, 8-story irregular torsion telecommunication building.....	46
Figure 4-3. Effect of structural period on floor acceleration amplification....	48
Figure 4-4. Effect of structural nonlinearity on the amplification of PFA	49
Figure 4-5. Effect of structural nonlinearity on the amplification of PFA	50
Figure 4-6. Effect of structural nonlinearity on the amplification of PFA	51

Figure 4-7 Comparison of floor acceleration-4-story irregular torsion building	54
Figure 4-8 Comparison of floor acceleration-8-story irregular torsion building	55
Figure 4-9. North / South, East / West Scaled 7 ground motions.....	58
Figure 4-10. Scaled response spectrum for 4story telecommunication building	60
Figure 4-11. Floor Response Spectrum for Irregular Torsion building	62
Figure 4-12. Floor Response Spectrum for 20-story SAC model building....	62
Figure 4-13. Floor response spectrum for irregular torsion building and 20- story SAC model building.....	63
Figure 4-14. Max acceleration demand for NSC located at 20-story SAC model building	65
Figure 4-15. Max acceleration demand for NSC located at irregular torsion building	65
Figure 5-1. Amplification of peak component acceleration of 20-story regular building	69
Figure 5-2. Amplification of peak component acceleration of 4-story irregular building	70
Figure 5-3. Typical behavior of non-structural component(FEMA E-74, 2011)	72

List of Tables

Table 2-1 Values of q_a for non-structural elements	24
Table 3-1. The comparison of the spectral acceleration and ESA acceleration	40
Table 3-2. Period and participation factor of buildings in case study	42
Table 3-3. Maximum amplification using spectral acceleration	43
Table 4-1. Torsional amplification factor (A_x) calculated at each story.....	53
Table 4-2. Scale factor for seven ground motions	59
Table 5-1. Seismic Coefficients for Mechanical and Electrical Components	67
Table 5-2. Response sensitivity classification of non-structural component (FEMA 274, 1997)	73
Table 5-3. Drift limits for deformation sensitive components (Gillengerten, 2001, 681-721)	74

Chapter 1 Introduction

Introduction

1.1. Research background

In the past two years, Gyeongju earthquake with a magnitude of 5.8 on the Richter scale (2016) and Pohang earthquake with a magnitude of 5.4 on Richter scale (2017) have occurred in Korea, causing irreversible property damage and raising awareness of the earthquake along with the fact that Korea is no longer a safe zone for earthquakes.

In particular, the earthquake has raised interest in the seismic design of non-structural components as well as the damage of structural elements such as beams, columns, and slabs. Although the architectural structural criteria stipulate that non-structural walls, double floors, ceilings and cabinets, which are not subject to structural resistance as well as structural elements, are also required to comply with the criteria, it is difficult to confirm the existence of actual application.

In this study, equivalent static approach for seismic design of nonstructural component was evaluated by using dynamic analysis that includes response spectrum analysis, and linear/nonlinear time history analysis. The result of dynamic analysis would be scrutinized in terms of torsion, higher mode effect, nonlinearity and roof level response by performing dynamic analysis.

1.2. Objectives and scope

Non-structural elements can undergo critical damages by ground motion intensity much lower than those required to damage structural components. Even though several significant non-structural damage were reported after the earthquake, most of them are neglected since there were no given design consideration. This phenomena leads the building to be habitable but no longer to be functional as shown in recent 2016 Kyungju earthquake and 2017 Pohang earthquake.(Figure 1-1)

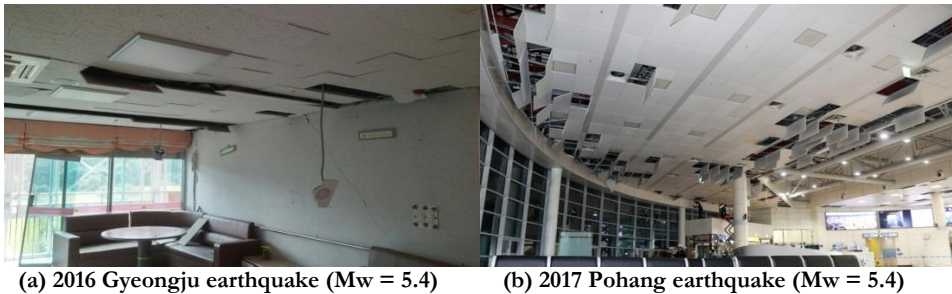


Figure 1-1 Non-structural damage due to Korean Earthquake (Lee et al, 2019)

The earthquakes occurred in Korea were just moderate earthquake with medium level of magnitude (Mw 5.4). However, the aftermath of earthquakes were costly because the building under the dynamic response critically amplifies ground motion for non-structural component located at the elevated portion of a building. Also, most buildings in Korea are not seismically sound considering building materials and structural details of the building.

The seismic design of non-structural component starts with understanding of difference between peak floor acceleration (PFA) and peak component acceleration (PCA). PFA is the maximum floor response demand

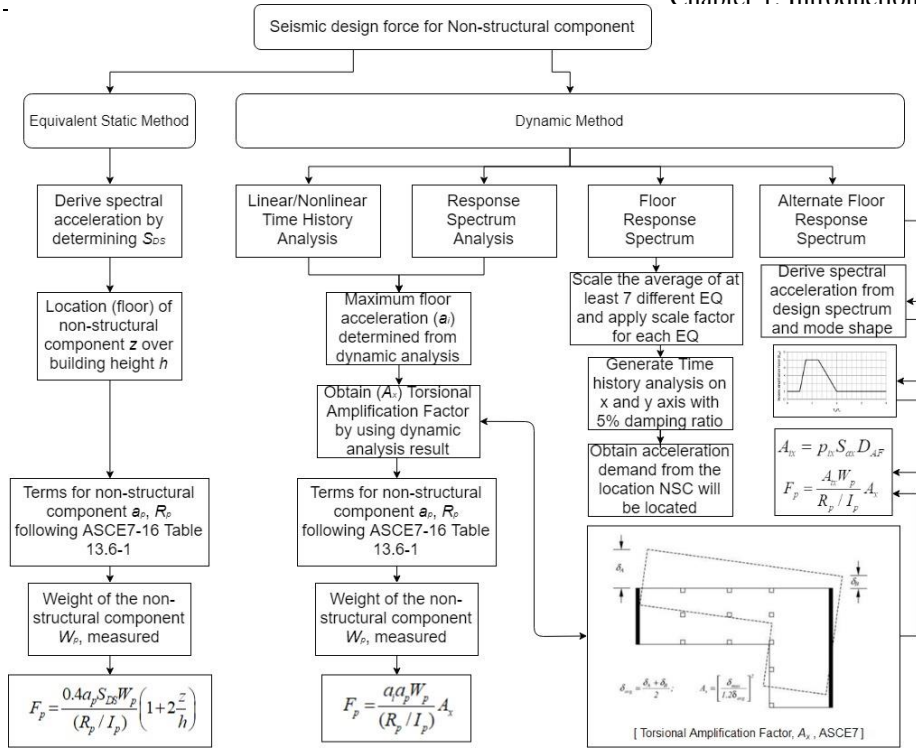


Figure 1-2. Flow chart for designing non-structural component (ASCE 7)

directly read from numerical analysis or the actual earthquake record. PCA is also the maximum response but it considers interaction between the building structure and non-structural element. In this study, PFA has been normalized by peak ground acceleration (PGA) to evaluate the amplification on each floor. Also, PCA has been normalized by PGA to check how much the interaction between non-structural component and the building structure influences actual earthquake load of non-structural component. But in order to calculate peak component acceleration, the first step is to figure out the peak floor acceleration to design non-structural component.

As shown in flow chart above, Figure 1-2, seismic design of non-

structural component is composed of equivalent static method and five different dynamic analyses, which are linear / nonlinear time history analysis, response spectrum analysis, floor response spectrum method and alternate floor response spectrum.

To briefly describe equivalent static load, the method was purposed to guarantee safety and practicality by simply using short period acceleration and elevation to calculate design seismic force. As a consequence, equivalent static method can overestimate or underestimate the seismic force in case of high rise buildings or irregular buildings. Therefore, the equivalent static method cannot represent the actual behavior of real structure. Rather than focusing on practicality, it is inevitable to appraise the method in terms of accuracy by investigating the building through several dynamic methods.

Many research for NSEs were conducted to develop rational seismic analysis methods such as Singh (1987), Villaverde (2004), Anajafi and Medina (2018). However, most studies are based on simplified two-dimensional numerical model that, in many cases, cannot represent real buildings characteristics (Anajafi and Medina (2018)). Since it is impractical to handle the correlation between structural and non-structural components using complex mathematics, the current code suggests equivalent static approach to simply maximize the practicality. However, the equivalent static approach fails to consider several key influences that greatly affect the acceleration demand on NSEs. Therefore, the equivalent static methods suggested by major building codes are critically reviewed through theoretical and numerical analysis and are evaluated to recommend possible

improvements.

1.3. Outline of thesis

This thesis contains five chapters.

Chapter 1 gave an introduction, objectives and scopes of this research work.

Chapter 2 reviews the current design codes and the previous studies on the static and dynamic approach of seismic design forces

Chapter 3 evaluates equivalent static load based on floor acceleration prediction based on structural dynamics

Chapter 4 discusses about numerical analysis result

Chapter 5 is the case study of R_p and a_p application

Chapter 6 is the summary and conclusion of thesis

Chapter 2 Review of Equivalent Static Approach in Design Standards and Previous Studies

2.1. Backgrounds of current design standards

2.1.1. 1994 NEHRP

As Singh (1993) proposed a new method of calculating the seismic force on non-structural component by using modal analysis approach, 1994 NEHRP incorporated the result of research by Singh. The method utilizes not only the first mode but also few first dominant modes to maximize the accuracy of the calculation. The code provides a complicated series of equations in which the acceleration of the roof is calculated based on the fundamental period of the building and the site acceleration (Kehoe (1998)). Further explanation follows in previous study section.

Simplified equation from 1997 UBC (shown in next section) is derived from 1994 NEHRP. The simplified equation is equivalent to UBC equation (2.4) but the equation (2.5) considering floor elevation effect is slightly different from 1997 UBC:

$$F_p = \frac{a_p A_p I_p W_p}{R_p}$$
$$A_p = C_a + (A_r - C_a) \left(\frac{x}{h} \right)$$
$$A_r = 2.0 A_s \leq 4.0 C_a \tag{2.1}$$

parameter for 1994 NEHRP is C_a , A_p , A_r and A_s . C_a is the peak ground

acceleration for short period building. A_p is component acceleration coefficient at point of attachment to the structure and A_r is component acceleration coefficient at structure roof level. Lastly, A_s is structure-response acceleration coefficient given below:

$$A_s = \frac{1.2C_v}{T^{2/3}} \leq 2.5C_a \quad (2.2)$$

where, C_v is seismic coefficient at grade as described in 1994 NEHRP provisions and T is an effective fundamental period of the structure.

2.1.2. 1994 /1997 UBC

In 1994 UBC, the code provides following equation for calculating seismic design force for non-structural components:

$$F_p = ZI_pC_pW_p \quad (2.3)$$

where W_p is the weight of the nonstructural element, Z is the seismic zone coefficient for the building. I_p is the importance factor for the nonstructural elements and C_p is the component amplification factor. Based on 1994 UBC, there are two values for C_p , 0.75 for most elements and 2.0 for elements behave like a cantilever. For C_p , higher value is recommended to guarantee the lack of recover capability of the element according to SEAOC (1990). Also, UBC afforded the suitable amplification factor for non-structural component with the fundamental period greater than or equal to 0.06 seconds.

For these elements, UBC recommends to increase the design force by a factor of 2.0 for resonance effect of the non-structural element. This factor does not take account for the amplification of the building relative to the ground (Kehoe (1998)).

1997 UBC provides two equations, and one of them can be generally used for non-structural components located anywhere in the building as given below:

$$F_p = 4.0C_a I_p W_p \quad (2.4)$$

This equation can be a practical way to calculate seismic design force, since F_p only relies on the type of non-structural component and the weight of it. However, this equation brings out conservative result that can result in unnecessarily over-estimated design. Therefore, after studies followed by Drake and Bachman (1995), UBC (1997) provided an equation that considers fundamental period of building and the site acceleration. Also, the acceleration of any floor level is then calculated based on linear distribution of acceleration over the height of the building. Simplified equation from 1997 UBC given below:

$$F_p = \frac{a_p C_a I_p}{R_p} \left(1 + 3 \frac{h_x}{h_r} \right) W_p \quad (2.5)$$

where a_p is the component amplification factor, C_a is the peak ground acceleration for short period buildings. R_p is the response modification factor for non-structural components, I_p is the importance factor for non-structural

components. h_x is the height of the floor to which the nonstructural element is attached and h_r is the height of the roof.

Same as current code provision, values for a_p varies between 1.0 for rigid elements and 2.5 for flexible elements. The modification factor R_p depends on the ductility of the support or anchorage of the non-structural element, which is provided by a table from UBC. Another important issue suggested by UBC 1997 is the upper and lower limit of the acceleration; $4C_a I_p W_p$ and $0.7C_a I_p W_p$ respectively, which is also shown in ASCE 7-16 equation.

2.2. Current design codes

In ASCE7-16, design guides for static and dynamic seismic design force, F_p was mainly developed by applying the force at the center of gravity and distributed relative to the component's mass distribution additional to the applied force calculated from seismic force equations. The recommendations of these works were also included in Korean Building Code and NEHRP provisions.

This section gives the basic information about various types of analyzing methods for nonstructural components, a range of applicability about dynamic analysis to evaluate the process of equivalent static analysis.

2.2.1. ASCE7-16

2.2.1.1. Equivalent static analysis

Typical floor spectrums for nonstructural components are calculated by

using seismic design force, F_p . According to ASCE7-16, static seismic force is defined by following equation:

$$0.3S_{DS}I_pW_p \leq F_p = \frac{0.4a_pS_{DS}W_p}{\left(\frac{R_p}{I_p}\right)} \left(1 + 2\frac{z}{h}\right) \leq 1.6S_{DS}I_pW_p \quad (2.6)$$

For parameters, F_p is a seismic design force to be applied at the center of mass and distributed along the component's mass distribution. I_p is the component's importance factor that varies from 1.0 or 1.5 and W_p is the operating weight of the non-structural component. z is the height to the top of the component with respect to the base of the building and h is the average roof height of structure with respect to the base. a_p is component amplification factor, which is given by ASCE7-16(2016) Table 13.4-1. Amplification factor is used for determining flexibility of building that becomes 1 for rigid component and 2.5 for flexible component. S_{DS} is 5% damped design spectral response acceleration which is given by ASCE7-16 Chapter 11.4.5 as given below:

$$S_{DS} = S \times 2.5 \times F_a \times 2/3$$

2.2.1.2. Dynamic analysis

Response spectrum analysis and Time history analysis

To check the applicability of torsional behavior, higher mode effects, nonlinearity and roof level response of a building, it is legitimate to compare floor spectra for both static and dynamic analysis. Moreover, this evaluation focuses on dynamic analysis of seismic design force for which is defined as

equation below:

$$0.5 S_{DS} I_p W_p \leq F_p = \frac{a_i a_p W_p}{\left(\frac{R_p}{I_p} \right)} \quad A_x \leq 1.6 S_{DS} I \quad (2.7)$$

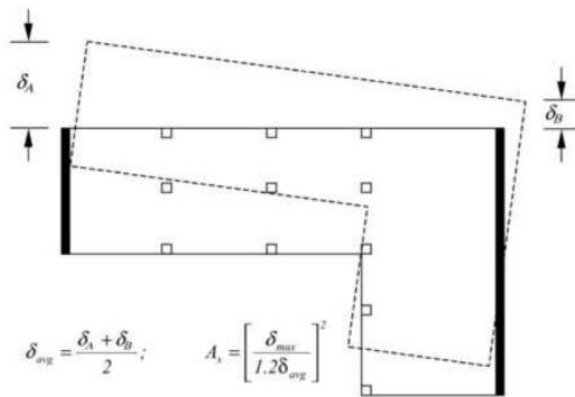


Figure 2-1 Torsional Amplification Factor A_x

where, a_i is the maximum acceleration at level i obtained from different dynamic analysis. A_x is the torsional amplification factor determined by equation below:

$$A_x = \left(\frac{\delta_{max}}{1.2 \delta_{avg}} \right)^2 \quad (2.8)$$

where, δ_{max} is the maximum relative displacement at level x computed assuming $A_x=1$ and δ_{avg} is the average of the displacement at the extreme points of the structure as shown in Figure 2-1:

The maximum acceleration at level i and torsional amplification

factor A_x can be estimated by performing numerical analysis based on linear dynamic analysis, nonlinear response history analysis, floor response spectra method and alternate floor response spectra method. In order to perform the linear and nonlinear time history analysis, it is required to select proper earthquakes that should be scaled and to perform time-consuming numerical integration. In practical terms, time history analysis is unnecessarily difficult and expensive to implement. To optimize the result and to consider several key influential parameters, response spectrum analysis is typically used to perform dynamic analysis for maximizing efficiency and economy.

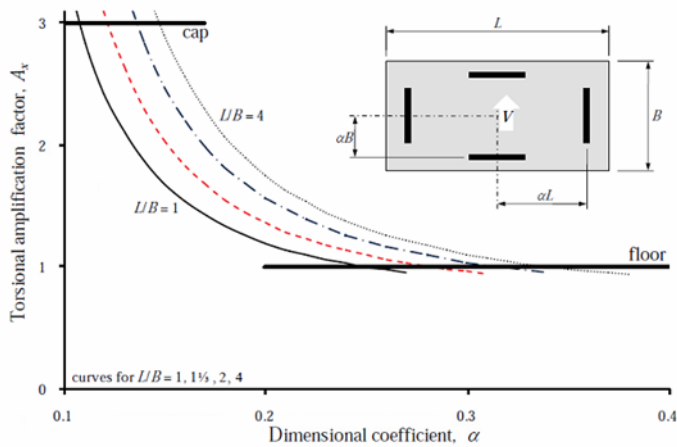


Figure 2-2. Amplification factor for symmetric rectangular buildings

Figure 2-2 illustrates the effect of equation (2.8) for a symmetric rectangular building with many different aspect ratio (L/B) (as shown in Figure 2-2) where the seismic force-resisting elements are positioned at a variable distance (defined by α) from the center of mass in each direction. Each element is assumed to have the same stiffness. The structure is loaded parallel to the short direction with an eccentricity of $0.05L$.

For α equals to 0.5, these elements are at the perimeter of the building, and for α equals to 0.0, they are at the center (providing no torsional resistance). For a square building ($L/B=1.00$), A_x is greater than 1.0 where α is less than 0.25 and increases to its maximum value of 3.0 where α is equal to 0.11. For a rectangular building with L/B equal to 4.00, A_x is greater than 1.0 where α is less than 0.34 and increases to its maximum value of 3.0 where α is equal to 0.15. (ASCE 7-16 commentary)

Floor response spectrum

As previously mentioned, there are four methods to evaluate dynamic approach; linear/nonlinear time history analysis, response spectrum analysis, floor response spectrum and alternate response spectrum analysis. Especially floor response spectrum method is the most straightforward among the other methods since it can be measured at the actual point that NSE will be located. Also, the method assumes that there is no interaction between the main structure and NSE, which allows component amplification factor to be 1 ($a_p=1$). This method has been widely used in nuclear engineering practice even though it has some decoupling process.

Floor response spectrum can be obtained by performing time history analysis using different sets of ground motion that are scaled to a target design response spectrum or artificial ground motions that are fitted to the design response spectrum. Another way to generate floor response spectrum is to read the response value straight from ground response spectrum. However, this method may cause a significant error that leads to relatively conservative

result because the response is obtained without considering interaction between the supporting structure and non-structural components.

The interaction effect becomes significant when the mass of non-structural component is not too small relative to the supporting structure and when the non-structural component is in tune with one of the predominant supporting structural period (Singh (1987)). Further explanation about interaction effect would be provided in previous study section.

Alternate floor response spectra.

To generate alternate floor response spectrum, the period of vibration and mode shapes of the structure should be calculated for at least three modes in each orthogonal direction using the modal linear dynamic analysis procedure. For each of the first three modes in each direction, the modal acceleration at each floor shall be calculated as a function of the nonstructural component period by following equation.

$$A_{ix} = p_{ix} S_{ai} D_{AF} \quad (2.9)$$

where, A_{ix} is the floor acceleration for mode x at level i , p_{ix} is the modal participation factor for mode x at level i obtained from the modal analysis. S_{ai} is the spectral acceleration for mode x , and D_{AF} is the dynamic amplification factor as a function of the ratio of component period to building period for

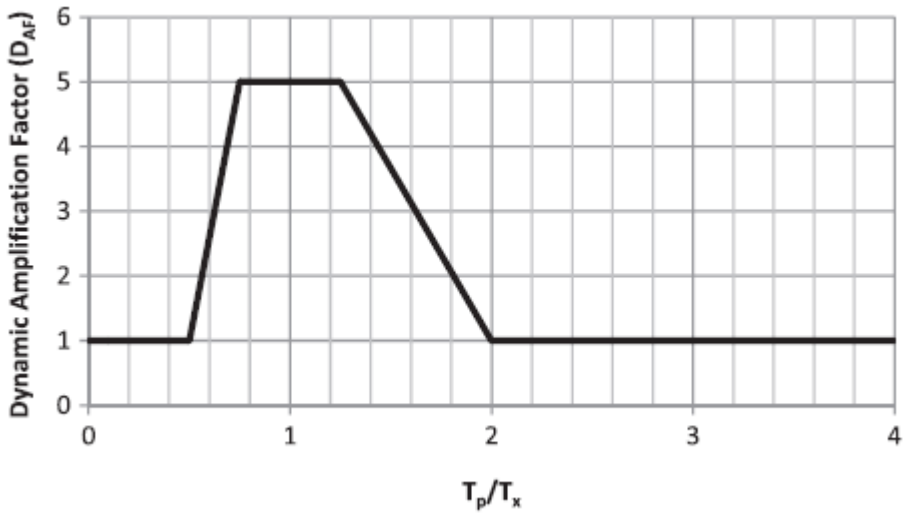


Figure 2-3 Component Dynamic Amplification Factor (D_{AF})

mode x from ASCE 7-16 Figure 2-3. To figure out dynamic amplification factor, each mode's period should be multiplied so that the factor for non-structural component can be computed to calculate the floor acceleration for mode x . The period of vibration, mode shapes and mode participation factors of the structure shall be calculated for at least the first three modes in each direction using modal analysis. In addition the floor response spectrum shall be taken as the maximum floor response acceleration at each building modal period also at least three modes, but not less than the spectral acceleration at the base of building.

Calculation of floor response spectra can be impractical since it requires time-consuming procedure of time history analysis. This method considers the dynamic amplification based on the behavior of first three modes of the structure to calculate the floor response spectrum. To generate alternate response spectrum it is necessary to be aware of dynamic properties

of both the building and non-structural components. Further explanation about alternate floor response analysis would be discussed in previous study section Kehoe (2003).

2.2.2. EUROCODE 8

Equivalent static analysis method for Eurocode 8 is given below:

$$F_a = (S_a \cdot W_a \cdot \gamma_a) / q_a \quad (2.10)$$

where, F_a is the horizontal seismic force, acting at the center of mass of the non-structural element in the worst case direction. W_a is the weight of the element and q_a is the behavior factor of the element from the Table 2-1 given by Eurocode 8.

Table 2-1 Values of q_a for non-structural elements

Type of non-structural element	q_a
Cantilevering parapets or ornamentations Signs and billboards Chimneys, masts and tanks on legs acting as unbraced cantilevers along more than one half of their total height	1.0
Exterior and interior walls Partitions and facades Chimneys, masts and tanks on legs acting as unbraced cantilevers along less than one half of their total height, or braced or guyed to the structure at or above their center of mass Anchorage elements for permanent cabinets and book stacks supported by the floor Anchorage elements for false (suspended ceilings and light fixtures)	2.0

γ_a is the importance factor of a non-structural component and lastly S_a is the seismic coefficient applicable to non-structural elements by using the given formula below:

$$S_a = \alpha \cdot S \cdot [3(1 + z/H) / (1 + (1 - T_a/T_1)^2) - 0.5] \quad (2.11)$$

where, α is the ratio of the design ground acceleration on type A ground, a_g , to the acceleration of gravity g and S is the soil factor. T_a is the fundamental vibration period of the non-structural element and T_1 is the fundamental vibration period of the building in the relevant direction. z is the height of the non-structural element above the level of application of the seismic action (foundation or top of a rigid basement) and H is the building height measured from the foundation or from the top of a rigid basement.

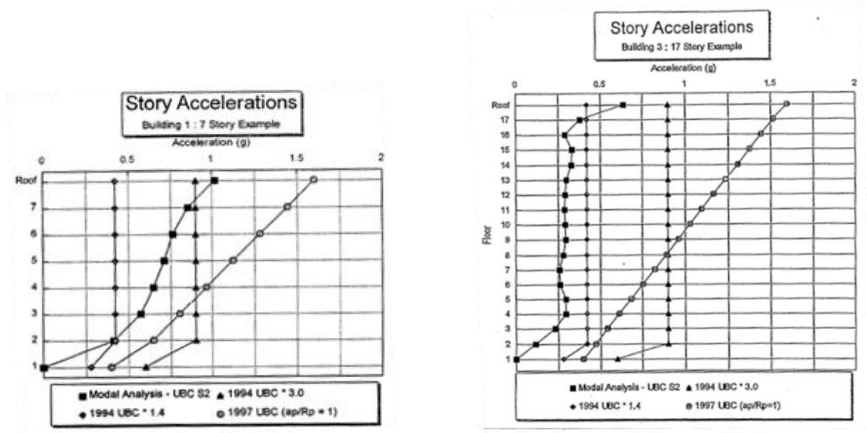
In Eurocode 8, both equivalent static method and dynamic method (floor response spectrum method) are proposed as in ASCE 7-16. The major difference between ASCE 7-16 and Eurocode 8 is that in Eurocode 8, the function of the fundamental period ratio between the component and the building influences component amplification. However, the application of equivalent static analysis on non-structural component is only applicable when both structural and nonstructural component's dynamic characteristic is known.

2.3. Previous studies

The improvement of cutting edge techniques for seismic analysis of non-structural component has been driven by the demand from nuclear power plant engineering over the past decades. The problem with accurately predicting the seismic performance of non-structural components is the

collaboration impact caused by the interaction between structural and nonstructural system. The direct modeling of the structural system results in excessive number of degrees of freedom and the large differences in mass, stiffness and damping values that causes impractical, uneconomic, and inaccurate mathematic calculation process.

2.3.1. Kehoe and Freeman (1998)



(a) 7 story example building

(b) 17 story example building

Figure 2-4 Comparison between 1994/ 1997 UBC, (Kehoe and Freeman, 1998)

1994 and 1997 edition of the Uniform Building Code were compared and criticized by Kehoe and Freeman (1998). They mentioned that 1997 edition of the UBC introduced linear distribution of design acceleration over

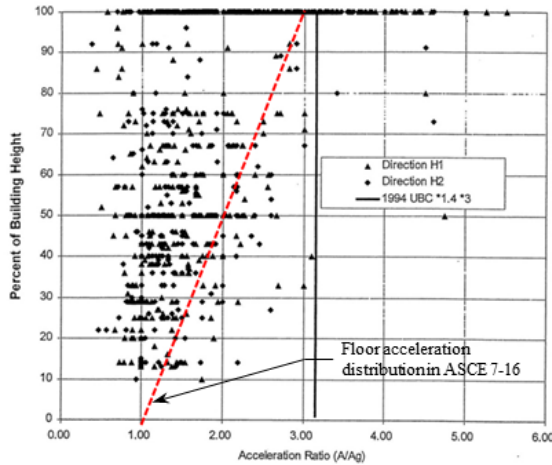


Figure 2-5 Instrumented building data (Drake and Bachman, 1995)

the height of the building. In this sense, equivalent static approach of ASCE7-16 seems to retain practical simplicity and consistency by using the instrumented building floor acceleration data obtained from California earthquakes. However, Kehoe and Freeman refer the problem of linear approach by saying that dynamic analysis result and data from instrumented building does not justify this change Kehoe and Freeman (1998). Therefore, it is necessary to evaluate equivalent static analysis method by using dynamic behavior of three dimensional buildings to check if the change in 1997 UBC is appropriate.

2.3.2. Drake and Bachman (1995)

Drake and Bachman (1995) analyzed the instrumented building data to derive the linear distribution of floor acceleration. As shown in Figure 2-5, amplification factor of three seems reasonable only for the typical floors. According to Drake and Bachman, equivalent static method from ASCE 7-16,

which brings out the maximum three times amplification of peak round acceleration (PGA) at the roof, does not follow linear distribution along the building height. Likewise for same approach, Villaverde (2004) insists that the equivalent static method does not consider the effect of inelastic behavior of the building.

2.3.3. Singh (1987)

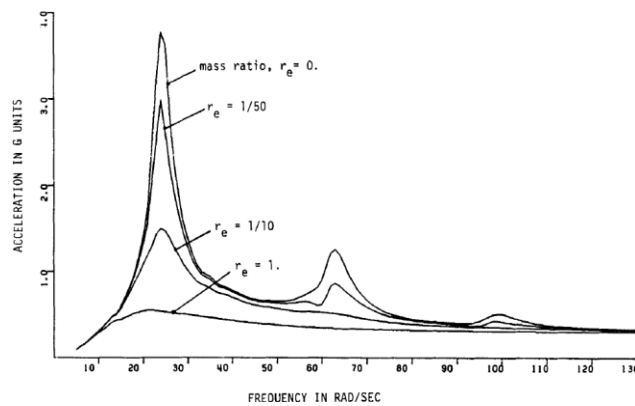
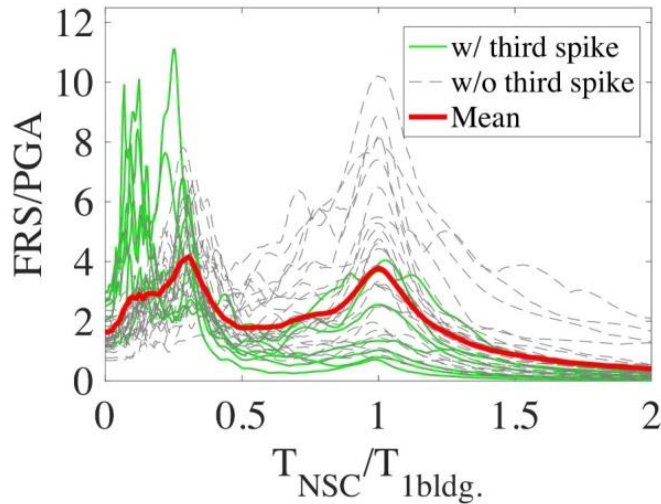


Figure 2-6 Floor response spectra corresponding different mass ratio (Singh, 1987)

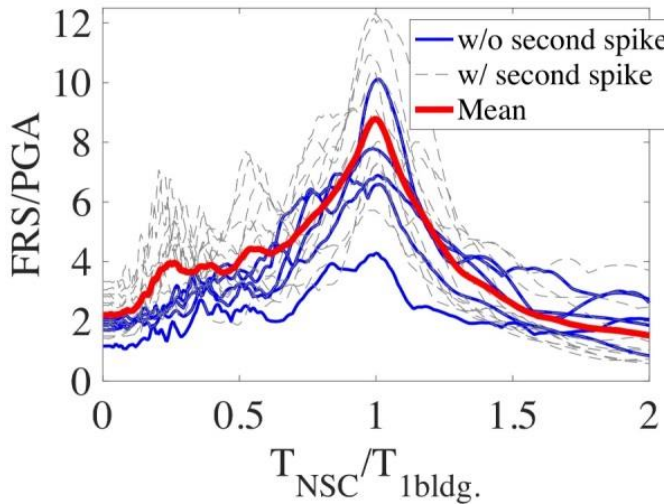
Singh (1987) states that it is essential to include the effect of the dynamic interaction between the equipment and supporting structure when the mass of non-structural component is not too small compare to supporting structure. He also emphasized the effect of modal behavior of the structure when the fundamental period of non-structural component is close to that of supporting structure. In case when the structural properties of structural and non-structural component are significantly different, the combined system

does not possess classical modes of vibration. Since also signifies that significant error can appear if non-classical damping effects are not considered.

2.3.4. Anajafi and Medina (2018)



(a) Moment resisting frame



(b) Shear wall system

Figure 2-7. 5% damped normalize roof spectra, (Anajafi and Medina, 2018)

Response of non-structural elements depending on lateral-load system

has been evaluated by Anajafi and Medina (2018). The paper refers that the response of non-structural elements can be different for two different lateral-load resisting system: moment resisting frame that are flexible and shear wall system that are rigid. Figure 2-7 shows that the peak component acceleration is larger in shear wall system compare to the moment resisting frame system. For high-rise moment resisting frame, tuned effect of non-structural elements is significant at higher mode.

Overall, this study demonstrates the significant influence of parameters such as the in-plane floor diaphragm flexibility, torsional responses of the supporting building, vertical irregularity in stories mass and stiffness, and the seismic base location in the estimation of non-structural components acceleration demands. This evaluation reveals that seismic demands for non-structural components are a function of the most salient characteristics of the supporting building such as lateral-load-resisting system, global ductility demand, and modal periods, as well as the ratio of non-structural component periods to building modal periods (tuning ratio)(Anajafi and Medina 2018).

2.3.5. Villaverde (2000)

Equivalent static method has been considered as conservative but simple method by Villaverde (2000). The method was derived on the basis of modal synthesis and the introduction of simplifying assumptions compare to design of supporting structure. Villaverde's main concern about equivalent static method is that the method should take influential parameters into account. Villaverde mentioned that the dynamic interaction between two subsystems should be considered and the level above the base of the structure

of the point and nonlinear behavior of structure with non-structural elements should be evaluated. Lastly, it used design spectra specified by building codes for the design of the structure as the earthquake input to the non-structural elements.

The major assumptions made in Villaverde (2000) for equivalent static method was the total response of the combined structure-non-structural system, which is approximately given by the response in the two modes of the system that correspond to the fundamental natural periods of the two independent subsystems. Furthermore, to assume worst case scenario, the fundamental natural period of the non-structural element coincides with the fundamental natural period of the structure (resonance effect). Also, the equation assumes linear distribution so that mode shape of the structure varies from zero at its base to a maximum value at the top. The damping ratio considered with equivalent linear system may be obtained by considering that the damping mechanism in the linear and nonlinear systems is approximately

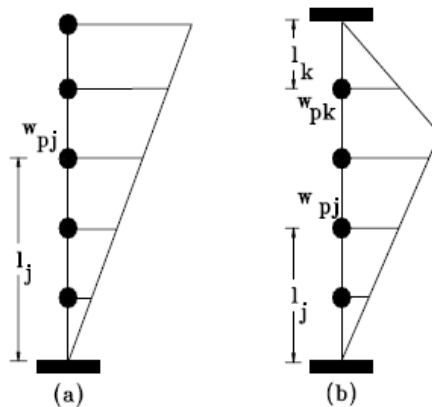


Figure 2-8. Assumed mode shapes for components with (a) one and (b) two points of attachment (Villaverde, 2000)

the same.

From the paper, Villaverde proposed linear distribution of maximum floor acceleration by using equation below:

$$F_{pj} = \frac{w_{pj}l_j}{\sum_{j=1}^n w_{pj}l_j} V_p \quad (2.12)$$

Where F_{pj} is the force acting at the center of the j^{th} mass of the non-structural element; w_{pj} is the weight of this j^{th} mass and l_j is the distance to the same mass measured in the case of a single attachment point from this attachment point (Figure 2-8). N is the total number of masses in the non-structural element and lastly V_p is the base shear of sum of the shears at the supports of the non-structural element given below:

$$V_p = \frac{IC}{\lambda} I_p C_p w_p \quad (2.13)$$

Other parameters were given above, but this equation introduces reduction factor for nonlinear behavior of the structure and non-structural elements by equation given below:

$$\lambda = \begin{cases} \mu_{eq} \\ \sqrt{2\mu_{eq}-1} \\ 1 + \frac{33-f}{25} (\sqrt{2\mu_{eq}-1}-1) \end{cases} \begin{cases} \text{if } (f \leq 2Hz) \\ \text{if } (2 < f < 8Hz) \\ \text{if } (8 \leq f \leq 33Hz) \end{cases} \quad (2.14)$$

where,

$$\mu_{eq} = \left[\frac{1}{N + n'} \left(\frac{N}{\mu} + \frac{n'}{\mu_p} \right) \right]^{-1} \quad (2.15)$$

Where, μ is the ductility factor for structure and μ_p is the ductility factor for non-structural component. N is the number of floors and n' is the number of resisting elements in the non-structural system. The reduction factor depends upon the frequency of the non-structural element.

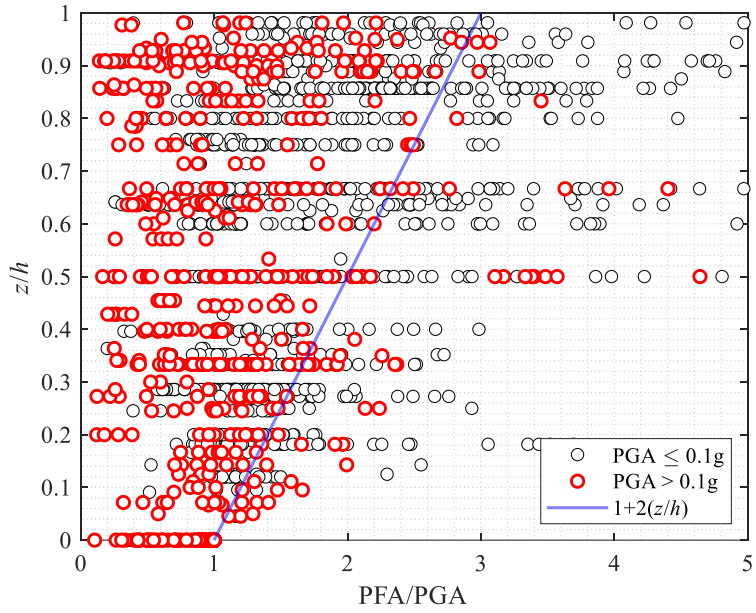
Chapter 3 Evaluation Based on Elementary Dynamic Theory

3.1. Introduction

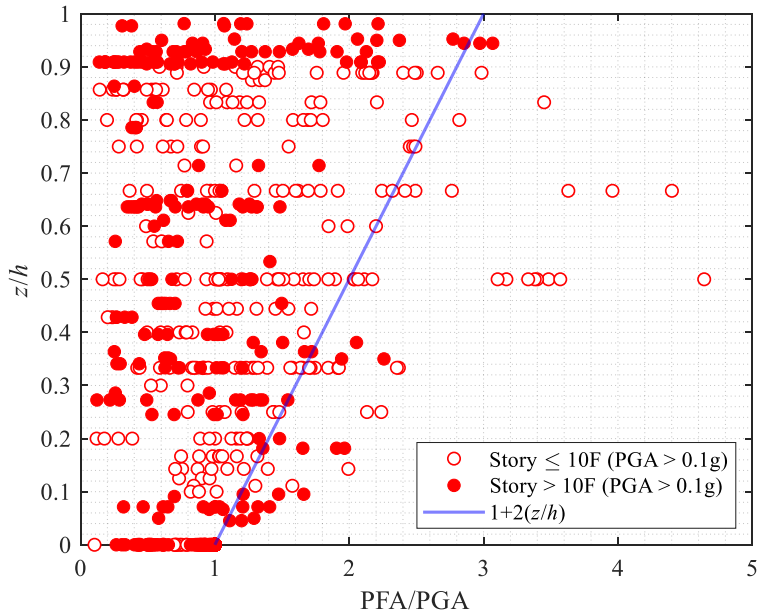
In this chapter, equivalent static load was evaluated based on several theoretical analyses that include floor acceleration prediction from elementary structural dynamics. Prior to perform numerical case studies and measure the floor acceleration data, the theoretical equation provides approximation process to anticipate basic flaws in current design code.

3.2. Preliminary analysis of instrumented building database

In most of cases, simplified numerical building models (such as two dimensional models) cannot represent the response characteristics of real buildings including flexibility of floor diaphragm, torsional response, real distribution of damage, contribution of infill and partitions, soil-foundation-structure interactions, damping effect, interaction between non-structural components and supporting structure (Anajafi and Medina (2018)). In order to analyze updated database of instrumented buildings, earthquake data from CESMD(Center for Engineering Strong Motion: www.strongmotioncenter.org) was handled as Drake and Bachman (1995) had done. The up-to-date database of instrumented buildings combines 63 earthquakes (1978 Santa Barbara (5.1 M_w), 1992 Landers (7.3 M_w), 1994 Northridge (6.4 M_w) and 2018 Thousand Palms (3.8 M_w)) measured from 66 buildings ranging from a single to a 54-story.



(a) All database



(b) Database with PGA over 0.1g

Figure 3-1. Peak floor accelerations as affected by PGA magnitude and building period

In Figure 3-1, the measured peak floor acceleration (PFA) is normalized to the peak ground acceleration (PGA) to be compared with linear approximation of ASCE 7-16. Figure 3-1 (a) demonstrates all data (around 3000 records) which shows different aspect of the peak floor distribution from Figure 2-5 Drake and Bachman (1995), which was as the empirical basis of the equivalent static design equation of ASCE 7-16. Figure 3-1 (a) also shows that for ground motion with higher intensity ($PGA > 0.1g$), the floor amplification got reduced because of nonlinear behavior of supporting structure. In Figure 3-1, (b), for buildings over 10-stories, peak floor acceleration is smaller than those in the lower story buildings because spectral acceleration has been reduced for longer period buildings. This preliminary analysis of instrumented building database clearly demonstrates that the up-to-date database does not accurately represent the magnitude and profile of the maximum floor acceleration specified by current equivalent static approach.

3.3. Absolute floor acceleration based on structural dynamics

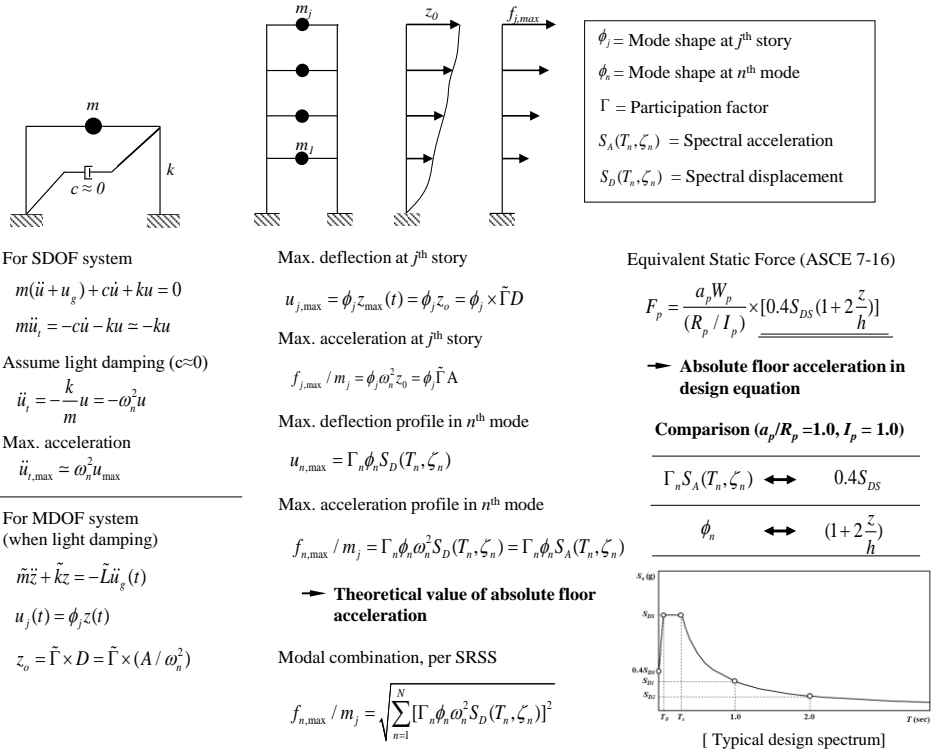


Figure 3-2 Summary of floor acceleration prediction based on elementary structural dynamics

In Figure 3-2, the derivation process for elementary structural dynamics Chopra (2007) is given. For calculation process, complicated process begins with simple single degrees of freedom system equation.

$$m(\ddot{u} + \ddot{u}_g) + c\dot{u} + ku = 0 \quad (3.1)$$

Above equation(3.1) refers behavior of one degree of freedom structure. By assuming light damping ($c \approx 0$), the equation becomes:

$$\begin{aligned}
 m\ddot{u}_t &= -c\dot{u} - ku \approx -ku \\
 \ddot{u}_t &= -\frac{k}{m}u = -\omega_n^2 u
 \end{aligned}
 \tag{3.2}$$

Response spectrum analysis shall not precisely estimate the value of maximum acceleration from the equation $-c\dot{u} - ku$. Thus, in structural analysis program, the maximum acceleration value is estimated by multiplying the square of natural frequency to the maximum displacement $\ddot{u}_{t,\max} = \omega_n^2 u_{\max}$.

Similarly, for multi-degrees of freedom system, under light damping, the equation becomes:

$$\tilde{m}\ddot{z} + \tilde{k}z = -\tilde{L}\ddot{u}_g(t)
 \tag{3.3}$$

And the displacement for each floor can be defined as:

$$u_j(t) = \phi_j z(t)
 \tag{3.4}$$

where, ϕ_j is the mode shape at j^{th} story and the maximum displacement can be determined by equation (3.5)

$$z_o = \tilde{\Gamma} \times D = \tilde{\Gamma} \times (A / \omega_n^2)
 \tag{3.5}$$

where, Γ is the participation factor for each mode and the displacement can be replaced by the acceleration value divided by the square of natural

frequency.

To define the maximum deflection at j^{th} story, two equations (3.4) and (3.5) should be combined to derive an equation (3.6).

$$u_{j,\max} = \phi_j z_{\max}(t) = \phi_j z_o = \phi_j \times \tilde{\Gamma} D \quad (3.6)$$

Similarly, the maximum acceleration at j^{th} story is defined as following:

$$f_{j,\max} / m_j = \phi_j \omega_n^2 z_o = \phi_j \tilde{\Gamma} A \quad (3.7)$$

The deflection profile due to the mode shape should be considered to theoretically prove the modal analysis. Similar to story deflection equation shown in equation(3.6), the maximum deflection profile in n^{th} mode shall be defined as below,

$$u_{n,\max} = \Gamma_n \phi_n S_D(T_n, \zeta_n) \quad (3.8)$$

where, $S_D(T_n, \zeta_n)$ is the spectral displacement depending on the frequency of each mode and the damping ratio.

The spectral acceleration can be derived by multiplying the square of natural frequency to the spectral displacement as defined below:

$$f_{n,\max} / m_j = \Gamma_n \phi_n \omega_n^2 S_D(T_n, \zeta_n) = \Gamma_n \phi_n S_A(T_n, \zeta_n) \quad (3.9)$$

This equation implies proportional aspect of the floor acceleration to the

squared natural frequency. Therefore, the higher mode effect can be significant even if the participation factor is smaller for higher modes. Therefore, the linear behavior of equivalent static analysis from ASCE 7-16 can over-estimate the maximum floor acceleration under higher mode effect. Additionally, the response spectrum analysis using the square root of the sum of the squares (SRSS) method is defined by modal combination equation below:

$$f_{n,\max} / m_j = \sqrt{\sum_{n=1}^N [\Gamma_n \phi_n \omega_n^2 S_D(T_n, \zeta_n)]^2} \quad (3.10)$$

Recalling equivalent static force equation from ASCE 7-16, equation (2.6), $0.4S_{DS}(1+2z/h)$ is the absolute floor acceleration in design equation. The comparison between the spectral acceleration derived from elementary structural dynamics and the floor acceleration from equivalent static force equation clearly shows that the maximum floor acceleration should be based on the spectral acceleration S_A instead of S_{DS} , which is short-period constant acceleration, because the structural modal behavior (structural period) has been considered for spectral acceleration when S_{DS} has not.

Table 3-1. The comparison of the spectral acceleration and ESA acceleration

Comparison ($a_p/R_p=1.0, I_p=1.0$)
$\Gamma_n S_A(T_n, \zeta_n) \Leftrightarrow 0.4S_{DS}$
$\phi_n \Leftrightarrow (1 + 2z/h)$

Newmark spectrum theory states that the spectral acceleration (S_A) is inversely proportional to structural period (T_a) when the structure belongs to the velocity-sensitive range. Therefore, when the structural period becomes longer, the floor acceleration would be much lower than ASCE 7-16 equivalent static result.

3.4. Response of non-structural element supporting structure's natural frequency

To evaluate maximum spectrum acceleration derived from previous section, roof level amplification of 1-, 10-, and 20-story were calculated using equation(3.7). Considering that $S_{D1} = S \times F_v \times 2/3$ and $S_{DS} = S \times 2.5 \times F_a \times 2/3$, S_{D1} becomes:

$$S_{D1} = \frac{S_{DS}}{2.5 \times F_a \times 2/3} \times F_v \times 2/3 = \frac{F_v / F_a}{2.5} \times S_{DS} \quad (3.11)$$

By using period of each building, the maximum acceleration was selected

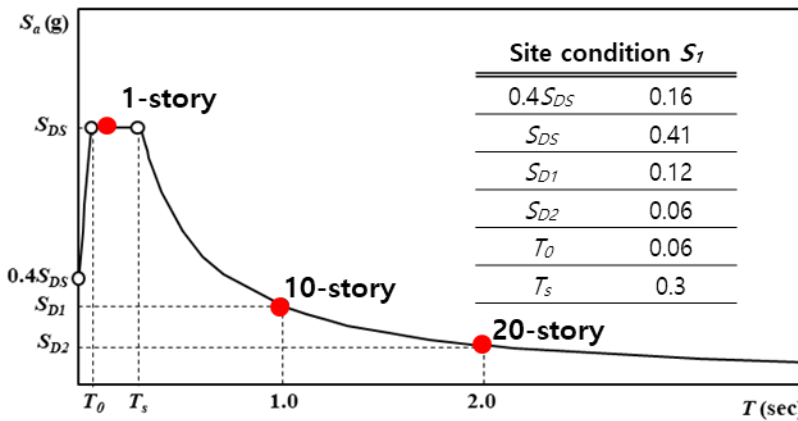


Figure 3-3 Response spectrum used to evaluate theoretical value of floor acceleration

from response spectrum Figure 3-3.

S₁ site condition was selected for case study with $F_a=1.12$ and $F_v=0.84$. The mode shape at the roof level is considered as 1.0 for comparison. Using equation (3.7), each result was normalized to $0.4 S_{DS}$ so that the maximum amplification factor for each building can be compared. Recalling equation (3.7), the period and participation factor are shown below:

Table 3-2. Period and participation factor of buildings in case study

$f_{jo} / m_j = \phi_{roof} \Gamma A_{max}$		
Story	Natural period, T_n (sec)	Participation factor (Γ)
1	0.1	1.0
10	1	1.3
20	2	1.45

Inputting natural period into design response spectrum draws S_{DI} value, which is the spectral acceleration. As previously mentioned, mode shape of the roof level is considered as 1.0 assuming that first mode governs. Participation factor is given in Table 3-2. By using equation(3.7), acceleration demands for each case can be calculated. In order to investigate each case study's floor amplification factor, the acceleration demand should be normalized by $0.4S_{DS}$. Normalizing each value by $0.4S_{DS}$ would draw the maximum amplification for each case.

The table below compares the maximum amplification of each building:

Table 3-3. Maximum amplification using spectral acceleration

Story	Maximum amplification
1	2.5
10	0.98
20	0.54

It is shown that the amplification of peak ground acceleration decreases as the period of supporting structure gets longer. (Period gets higher when the height of the building gets higher) This occurs because low-rise building belongs to acceleration sensitive region and mid to high-rise building belongs to velocity sensitive region.

3.5. Summary

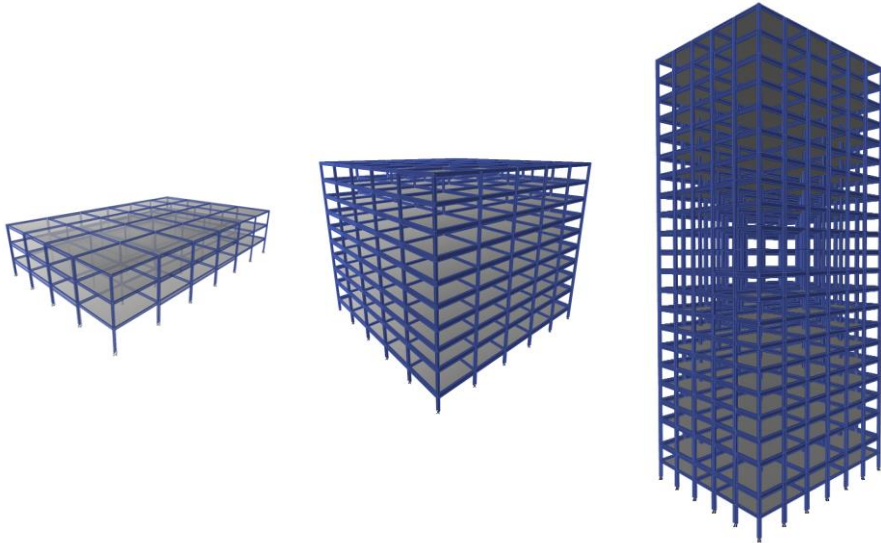
To make numerical analysis more reliable, theoretical analysis provides more clear understanding of the contribution of higher mode effect. Consideration of higher mode had become more essential because natural frequency influences the maximum acceleration although participation factor for higher mode is small. Evaluation of the floor acceleration from equivalent static force equation, compare to the spectral acceleration derived from theoretical analysis, clarifies that the maximum floor acceleration should be based on spectral acceleration S_A instead of S_{DS} since spectral acceleration considers the structural modal behavior when S_{DS} does not.

Chapter 4 Evaluation of Equivalent Static Method based on Numerical Analysis

4.1. Introduction

This chapter evaluates the equivalent static approach by understanding numerical analysis based on dynamic behavior of several supporting structural characteristics on the response of floor acceleration. A total of five three-dimensional models were evaluated using structural analysis program. There are two parts of analysis, the first part explains the dynamic behavior of 3-, 9-, 20-story SAC building models that are designed based on UBC (1994) for Los Angeles area Gupta and Krawinkler (1999), and the second part explains the dynamic behavior of 4- and 9-story telecommunication center buildings. The first part investigates the effect of structural period, higher modes, and structural nonlinearity and the second part examines the amplification of floor response due to the torsional effect by analyzing asymmetrical buildings that also includes the effect of structural period and nonlinearity.

4.2. Numerical model: 3-, 9-, 20-story SAC model, 4-, 8-story telecommunication building model



(a) 3-story building (b) 9-story building (c) 20-story building

Figure 4-1 Three SAC building models designed according to UBC 1994

Eigenvalue analysis of three SAC buildings (Figure 4-1) draws the fundamental periods of each building; 1.16 sec (3-story), 2.37 sec (9-story) and 3.87 sec (20-story) respectively. For dynamic analysis, response spectrum analysis using UBC 1994 design spectrum with 100/30% bi-directional loading and time history analysis by inputting two sets of ground motions (Sylmar, 1994 and Imperial Valley, 1940) were applied. Imperial Valley ground motion is typically considered as standard earthquake to evaluate a building because the earthquake has a sufficient time duration and moderate epicentre distance. On the other hand, Sylmar earthquake is close to pulse-type excitation with short epicentre distance. Both earthquakes were scaled to UBC 1994 design response spectrum compatible for each building's period with seismic zone factor 0.4 in zone 4 and site coefficient S_2 . Plastic hinges of

each building were assigned at beam ends as a point hinge with a bilinear moment-rotation relationship with 3% strain hardening effect. Plastic hinge modelling parameters were determined by following ASCE 41-13.

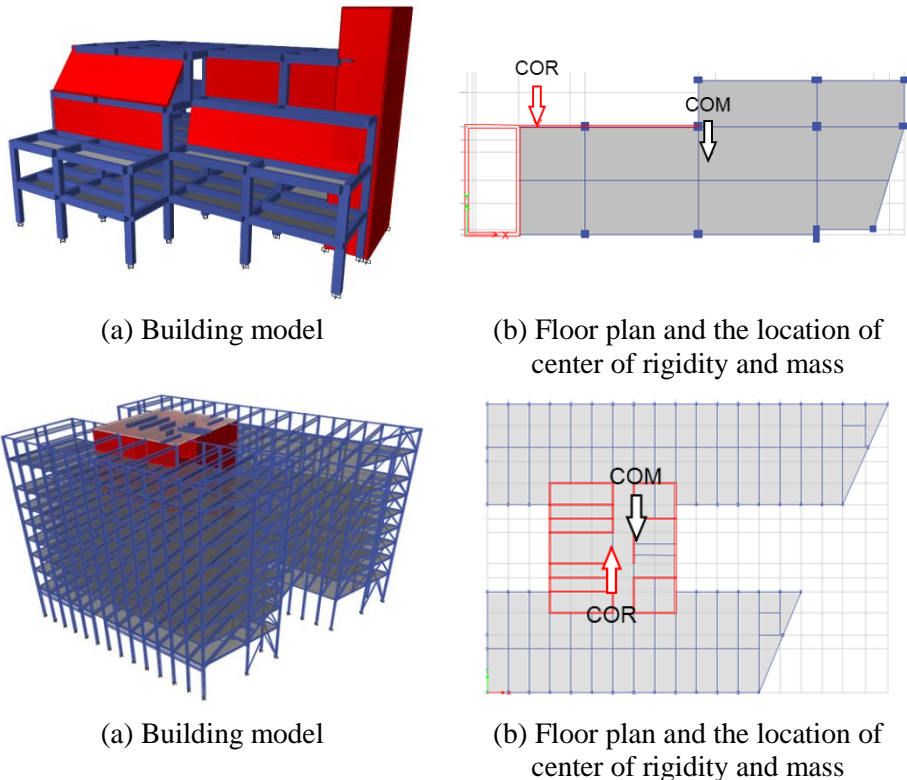


Figure 4-2 4-, 8-story irregular torsion telecommunication building

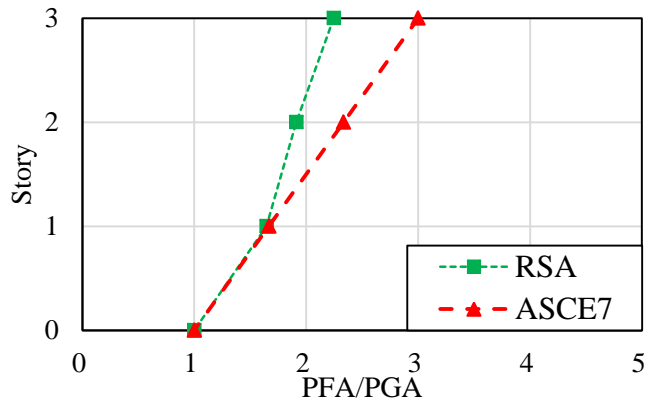
4.3. Effect of structural period

Figure 4-3 demonstrates the response spectrum analysis result. Each floor's acceleration was normalized to the effective PGA, which is $0.4S_{D5}$. As shown in figure, equivalent static approach equation is only comparable to 3-story building result. The behavior of 9-story and 20-story buildings indicates that the equivalent static method overestimates the actual floor acceleration.

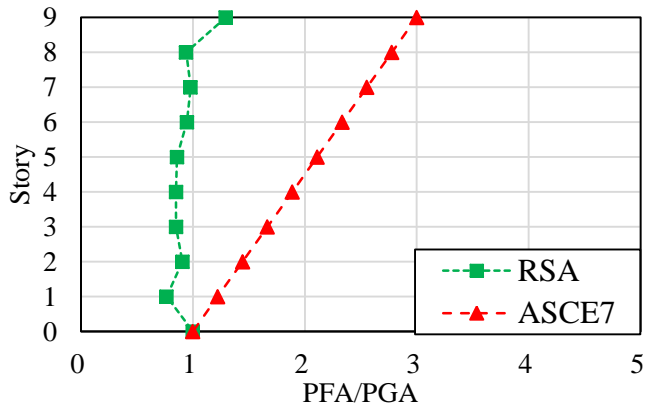
This result implies the floor acceleration is overly estimated by the equivalent static method as the fundamental period of buildings increase. Theoretical analysis in previous section also mentioned that when the structural period becomes longer, the floor acceleration would be much lower than ASCE 7-16 equivalent static result.

4.4. Effect of higher modes

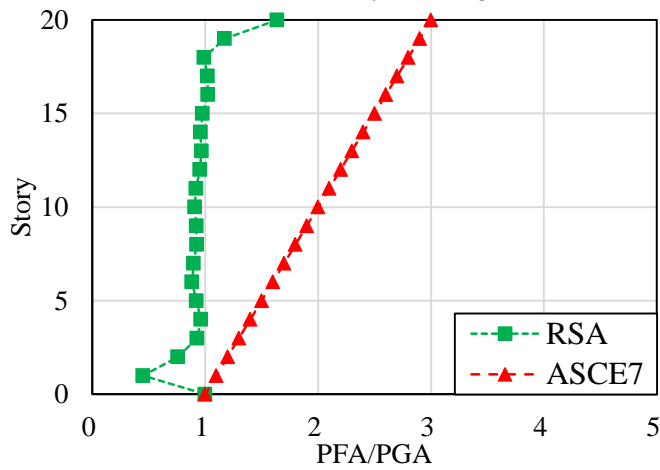
Higher mode effect of buildings with higher fundamental period were predicted by Figure 4-3 (b) and (c). The floor accelerations are almost constant along the height of the building except for the top and bottom floor due to higher mode effect. This phenomenon occurs because higher mode effect weakens the effect of first mode, which is typically the governing mode. The derivation from chapter 4.1 defines higher mode effect by emphasizing the effect of structural period with lower floor acceleration compare to the floor acceleration from equivalent static approach. Also, the previous study by Kehoe and Freeman (1988) shows the similar aspect by using two dimensional models (Figure 2-4).



(a) 3-story building

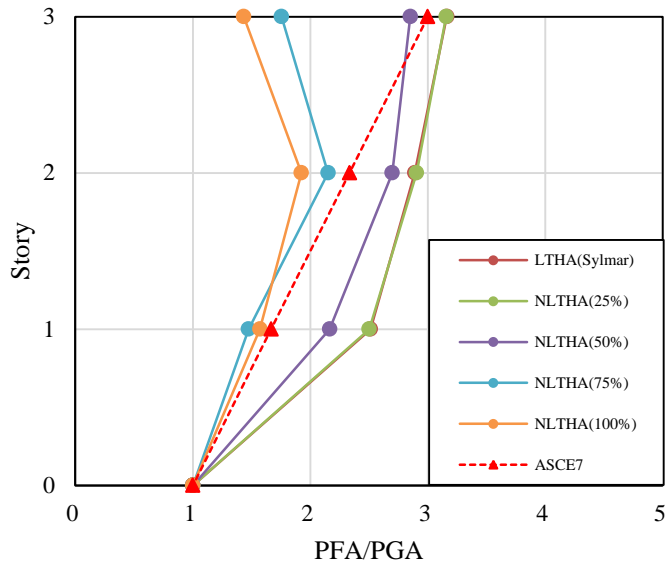


(b) 9-story building

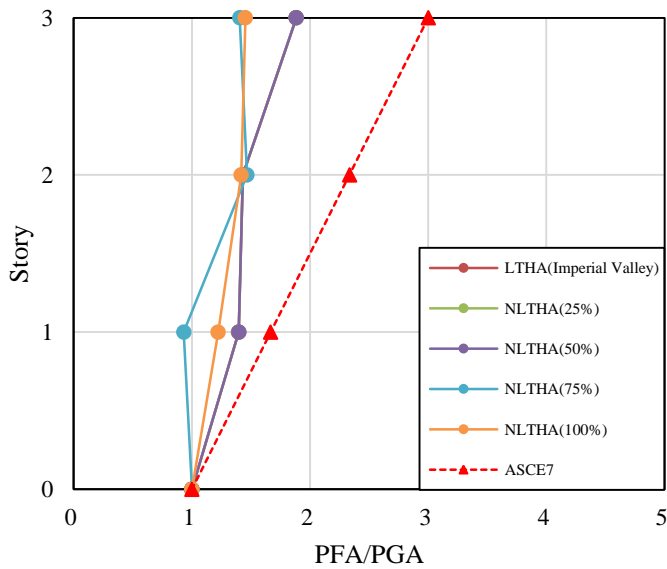


(c) 20-story building

Figure 4-3. Effect of structural period on floor acceleration amplification

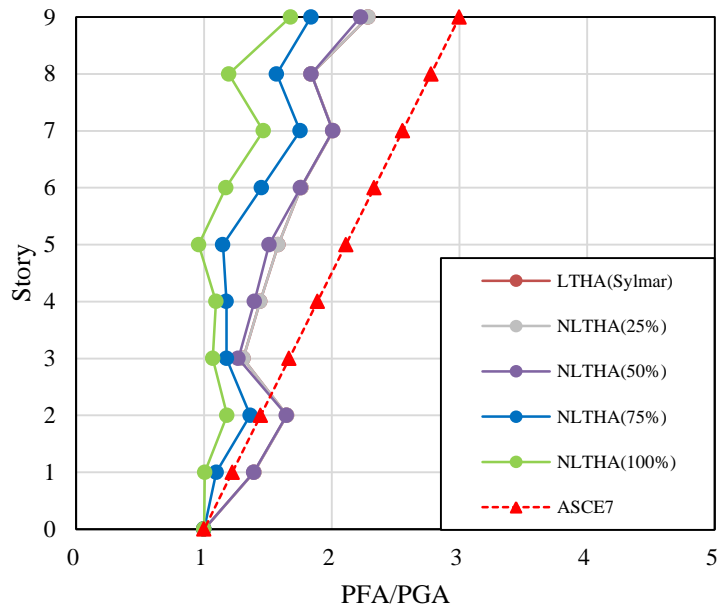


(a) Sylmar earthquake

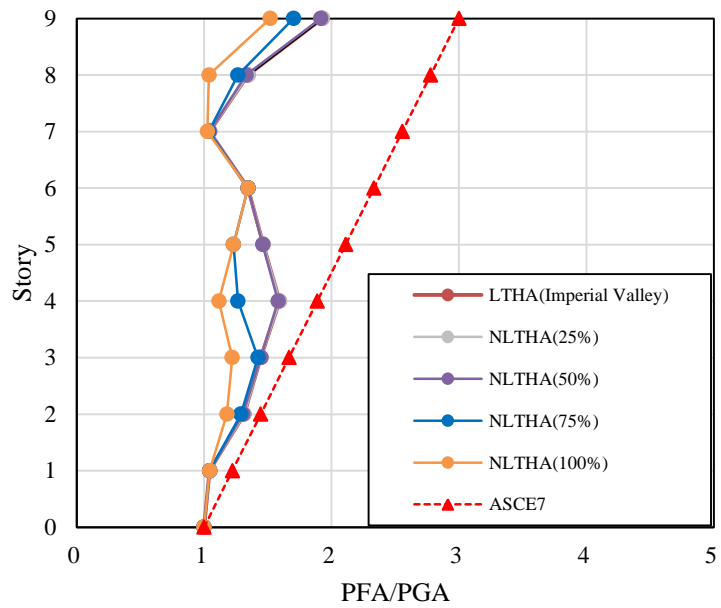


(b) Imperial valley earthquake

Figure 4-4. Effect of structural nonlinearity on the amplification of PFA (3-story SAC model)

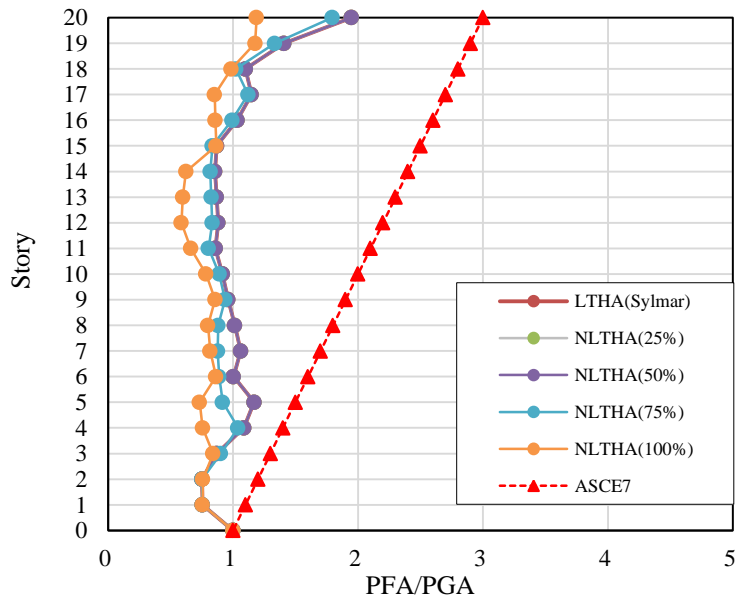


(a) Sylmar earthquake

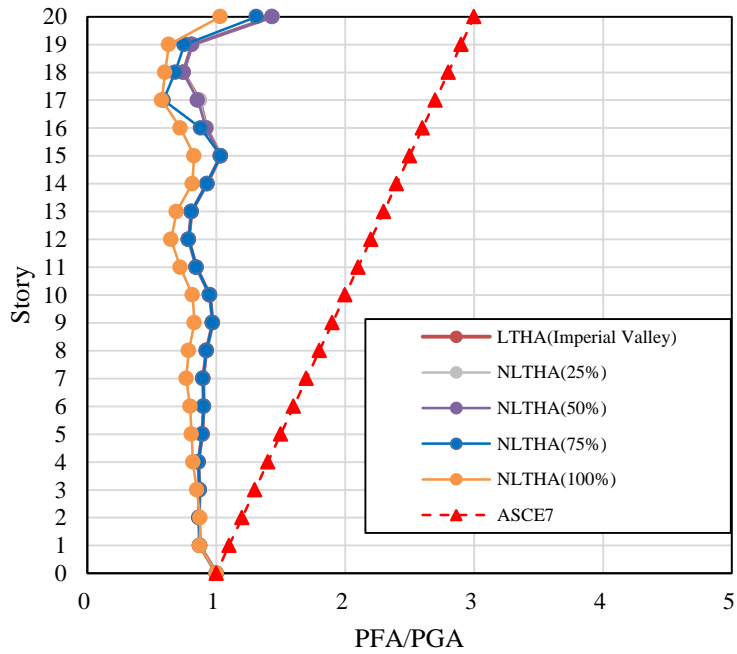


(b) Imperial valley earthquake

Figure 4-5. Effect of structural nonlinearity on the amplification of PFA (9-story SAC model)



(a) Sylmar earthquake



(b) Imperial valley earthquake

Figure 4-6. Effect of structural nonlinearity on the amplification of PFA
(20-story SAC model)

4.5. Effect of Nonlinearity

The result of nonlinear time history analysis for 3-, 9-, 20-story SAC building were shown in Figure 4-4, Figure 4-5, Figure 4-6 respectively. By controlling the intensity of ground motion, the behavior of structure depends on degrees of nonlinearity has been evaluated. The ground motion intensity up to 50% did not cause significant nonlinear behavior of structure. As the ground motion higher than 50% applied, the floor accelerations of both 9-, and 20-story building were reduced due to the nonlinearity. However, non-structural element located inside the building might experience higher acceleration demand if one of the dominant natural frequencies of the supporting structure shifts into the natural frequency of non-structural element as Singh (1987) emphasized in his study.

4.6. Torsion

4.6.1. Introduction

This section provides the influence of building torsional irregularity on the floor acceleration. In order to evaluate the equivalent static approach in terms of torsional behavior of a structure, as Figure 4-2 illustrates, 4-, 8-story irregular torsion telecommunication buildings were used for evaluation. The fundamental period obtained from eigenvalue analysis was 0.497sec for the 4-story building and 0.482sec for the 8-story building. The center of rigidity (CR) and the center of mass (CM) are shown in Figure 4-2. The distance between the center of rigidity and the center of mass of 4-story and 8-story buildings are 40.5% and 6.8% respectively measured by the ratio of the distance between CR and CM and the length of the building perpendicular to

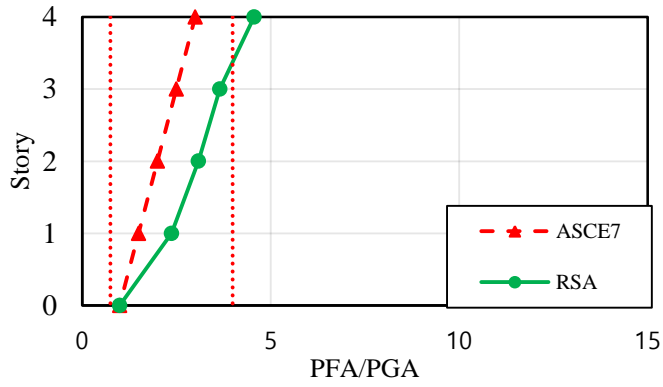
the direction which response spectrum analysis. Since the 4-story building has far distance between CM and CR, the building is expected to experience very severe torsional irregularity than the 8-story steel building with centered core wall.

4.6.2. Evaluation of ASCE 7-16 method

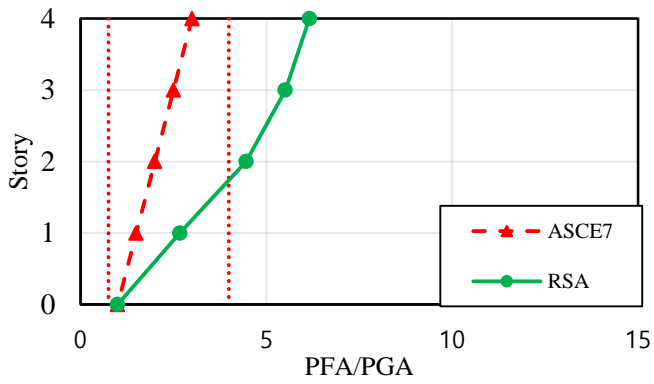
Again, for 4-, and 8-story irregular torsion building, response spectrum analysis performed to check the torsional effect on floor acceleration. KBC2016 design response spectrum for S_c site class, which was suggested by structural calculation of telecommunication building. Spectral acceleration for the design response spectrum follows structural calculation as well. Bi-directional analysis (30/100 rule) was performed to compute the torsional mode of vibration effect. As shown in plan view of both buildings Figure 4-2(b), the relatively far distance between the center of mass and center of rigidity refers irregular torsional behavior of two buildings. Therefore, in this case, torsional amplification factor value should be significant compare to the previous cases. The torsional amplification factors according to equation (2.8) for two buildings are summarized in Table 4-1. As expected the 4-story building has very high torsional amplification factor over 2.5.

Table 4-1. Torsional amplification factor (A_x) calculated at each story

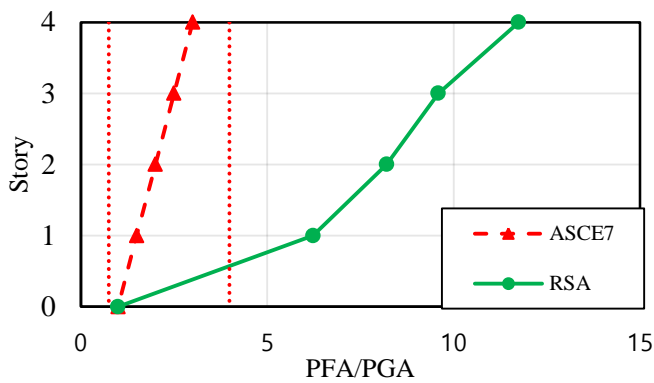
	1	2	3	4	5	6	7	8	9
4-story building	1.00	2.63	2.66	2.62	2.57	-	-	-	-
8-story building	1.00	1.35	1.27	1.22	1.18	1.14	1.10	1.07	1.01



(a) $a_{i,max}/PGA$

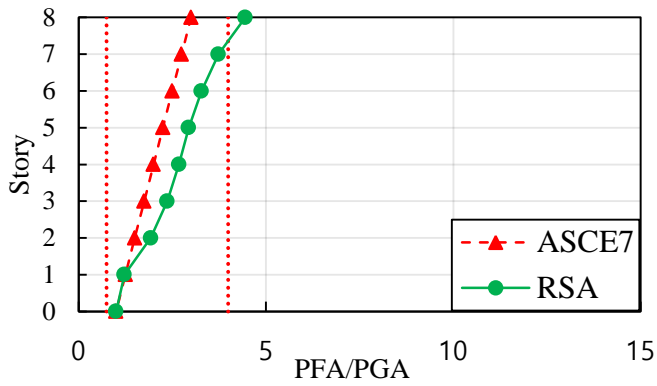


(b) $a_{i,CR} \cdot A_x / PGA$

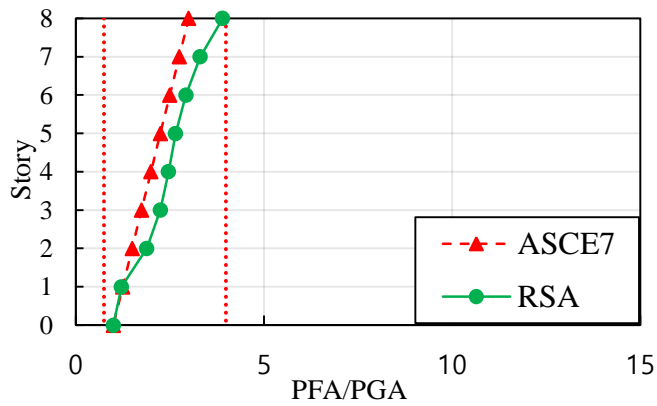


(c) $a_{i,max} \cdot A_x / PGA$

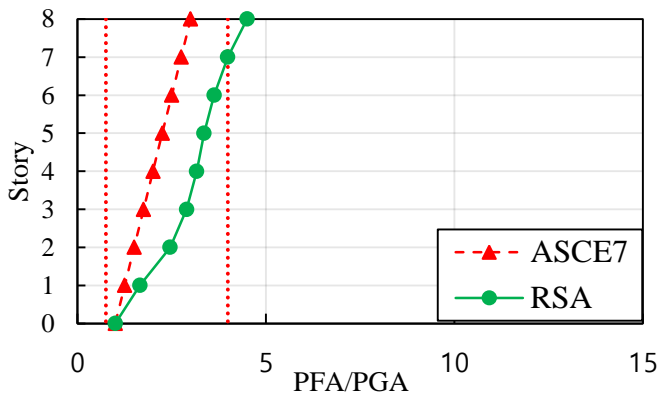
Figure 4-7 Comparison of floor acceleration-4-story irregular torsion building



(a) $a_{i,max}/PGA$



(b) $a_{i,CR} \cdot A_x / PGA$



(c) $a_{i,max} \cdot A_x / PGA$

Figure 4-8 Comparison of floor acceleration-8-story irregular torsion building

Figure 4-7, Figure 4-8 compares the maximum floor acceleration plotted based on three different cases: (a) $a_{i,max}$, the direct maximum acceleration output from structural analysis program, (b) $a_{i,CR} \cdot A_x$, the acceleration output from the center of rigidity of each floor amplified by the torsional amplification factor (A_x) and (c) $a_{i,max} \cdot A_x$, the maximum floor acceleration output from program amplified by torsional amplification factor, which can be a misleading interpretation of dynamic approach in ASCE7-16. Using the original approach defined by ASCE7-16 (Case (c)) can result in the erroneous application of equation (2.7) and derive a huge overestimation of the floor acceleration due to the severe torsional irregularity. (Figure 4-7(c)) Therefore, such application should be avoided.

Instead, the correct way to apply ASCE7-16 dynamic analysis (Case (b), Figure 4-7(b)) draws somewhat conservative result compare to exact maximum acceleration value (Case (a), Figure 4-7(a)) for 4-story building with severe irregularity. On the other hand, the 8-story building with minor irregularity does not follow the same trend as the 4-story building (Figure 4-8). For 8-story building, all three cases show the similar behavior because torsional amplification factor is close to 1, which means torsional effect due to irregularity is relatively low. Compare to dynamic analysis result for 8-story, the equivalent static analysis gives more reasonable result since acceleration value for 8-story building indicates the behavior of regular building with relatively short fundamental period (0.482sec).

If possible, the value at the point farthest from the center of rigidity (output of structural analysis program result) should be read regardless of the

torsional irregularity. Nonetheless, there are some engineering judgement needs to be considered whether $a_{i,max}$ or $a_{i,CR}$ value to be used for floor acceleration determination. For instance, in equation(2.7), A_x can only be used when a_i is selected at the center of rigidity instead of the maximum floor acceleration and also for non-structural elements located far from the center of rigidity. Likewise, when the non-structural element located at the center of rigidity $a_{i,CR}$ can be justified. Anyhow, $a_{i,max}$ can be used for conservative design of non-structural component.

4.7. Floor response spectrum method application

Floor response spectrum method draws realistic value for determining acceleration demands because actual acceleration value is obtained (either can be the maximum acceleration for conservative design or at the location where non-structural component would be placed). Using 20-story SAC model from Figure 4-1 and 4-story telecommunication building model from Figure 4-2, floor response spectrum approach has been conducted.

The seven ground motions that are suitable to KBC response spectrum were chosen from PEER Ground Motion Database. Ground motions are listed in Table 4-2.

In order to conduct floor response spectrum, the numerical model should be analyzed by time history analysis. To perform time history analysis, it is necessary to design and correct ground motions according to KBC 17 7.3.4.1. Each ground motions are composed of two directions, x and y. (Figure 4-9)

To determine scale factor for optimal scaled ground motions (Table 4-2), the acceleration at the location of non-structural component is needed. The

conservative way to determine seismic force is to read maximum floor response at the floor. The response spectrum should be derived based on maximum floor motion at the floor and the response spectrum under 5%

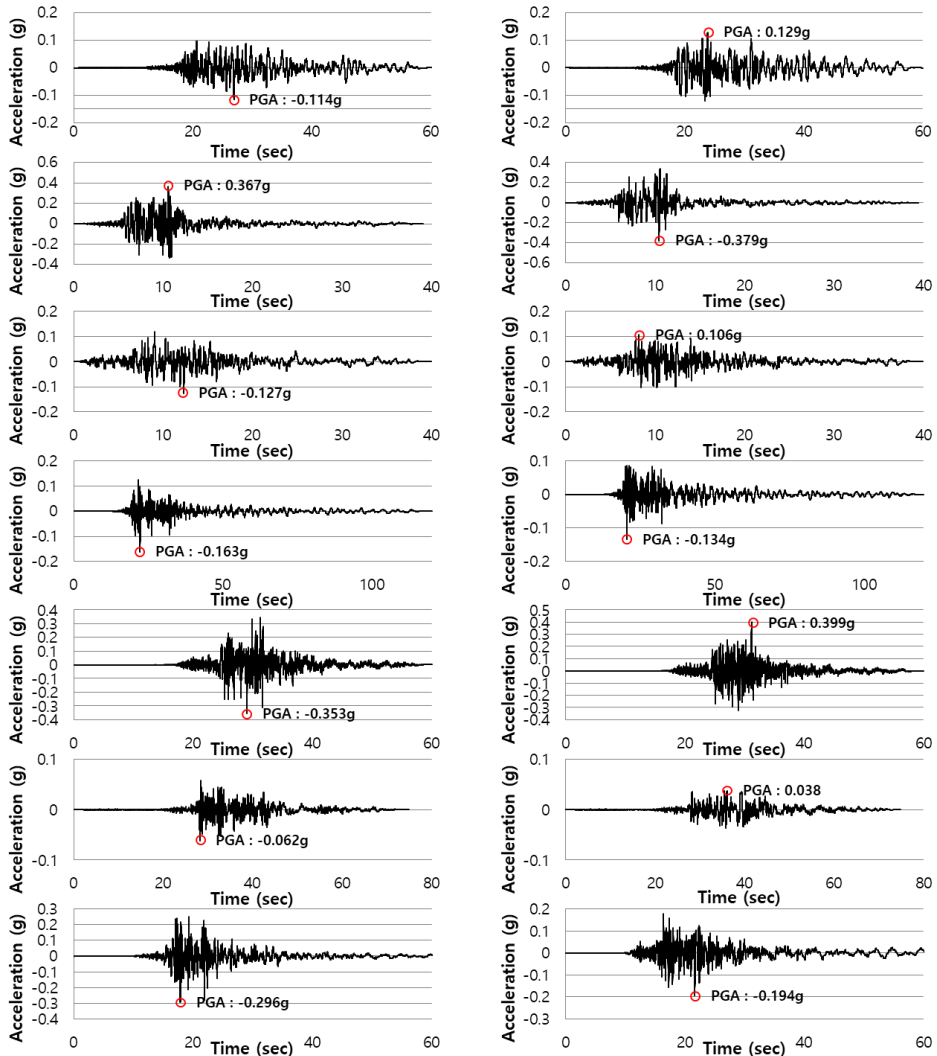


Figure 4-9. North / South, East / West unscaled 7 ground motions

damping should be derived using square root of sum of the squares (SRSS)

Table 4-2. Scale factor for seven ground motions

Name of seven EQs	Scale Factor	Scaled range (sec)
Chuetsu-oki - Sanjo	0.841	0.10 ~ 0.78
Imperial Valley - El Centro Array #11	0.618	
Loma Prieta - Fremont - Mission San Jose	1.625	
Chuetsu-oki - Niigata Nishi Kaba District	0.903	
Iwata_Japan - Misato_Miyagi Kitaaura - A	0.805	
Chi-Chi_Taiwan-03 - TCU070	1.741	
Kobe_Japan - Tadoka	0.970	

method for each ground motion

After deriving seven different response spectrums from seven ground motions, it is simple to find optimal scaling factor by using following equation from Dynamics of Structure (Chopra, 2018):

$$SF_{opt} = \left[\prod_{i=1}^{n_p} \frac{A_{CMS}(T_i)}{A(T_i)} \right]^{1/n_p} \quad (4.1)$$

where, A_{CMS} is the design spectrum multiplied by 1.3 and 0.9, $A(T_i)$ is the acceleration value for each response from ground motions and n_p is the number of data of response spectrum in a range of interest. The range of interest should be determined by:

$$0.2 \times T_o < T < 1.5 \times T_o \quad (4.2)$$

The average of the response spectrum of seven ground motions should be scaled by a scaling factor based on Chopra applied to minimize the difference between design response spectrum and the average of seven ground motions. The design spectrum and the 1.3*design spectrum are illustrated in the Figure 4-10 along with the SRSS spectra of the seven scaled ground motions. 0.2 times of the relatively short x-direction primary mode period and 1.5 times of the relatively long y-direction primary mode period are shown together, and the average SRSS spectrum of the scaled ground motions in the corresponding interval satisfies the target response spectrum. The adjusted seven pairs of seismic time histories are shown in the Figure 4-10.

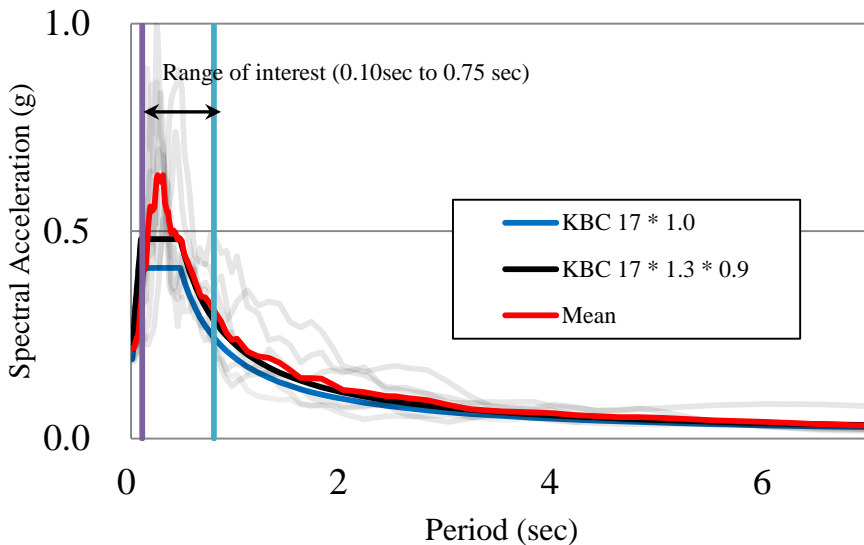


Figure 4-10. Scaled response spectrum for 4-story telecommunication building

For two cases, 4-story irregular torsion building and 20-story SAC model, max floor response spectrum is obtained at the top floor. Only 4-story irregular torsion building case has been shown for demonstration because it is a same process for both cases. As mentioned in Figure 4-4, Figure 4-5, Figure

4-6, nonlinearity of structure typically lowers the floor acceleration demand during the ductile process. For conservative result, floor response spectra are obtained under the assumption that a structure and its NSEs behave as linear systems. (see Figure 4-11, Figure 4-12)

Figure 4-11 demonstrates the floor response spectrum of irregular torsion building at the joint with maximum floor motion. Figure 4-12 is the maximum floor response spectrum for 20-story SAC model building with minimized torsional effect. It clearly shows that the acceleration demand at the irregular torsional building is much higher than that of 20-story SAC model building.

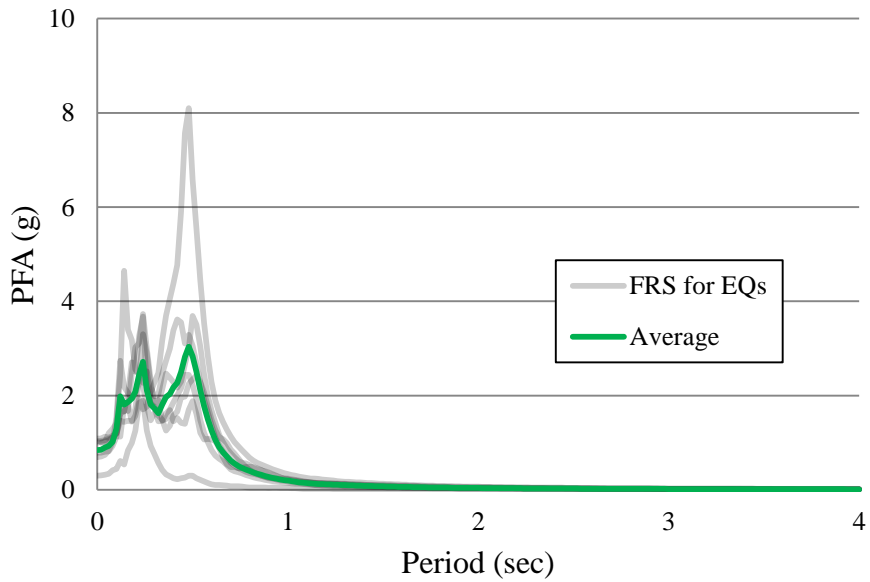


Figure 4-11. Floor Response Spectrum for Irregular Torsion building

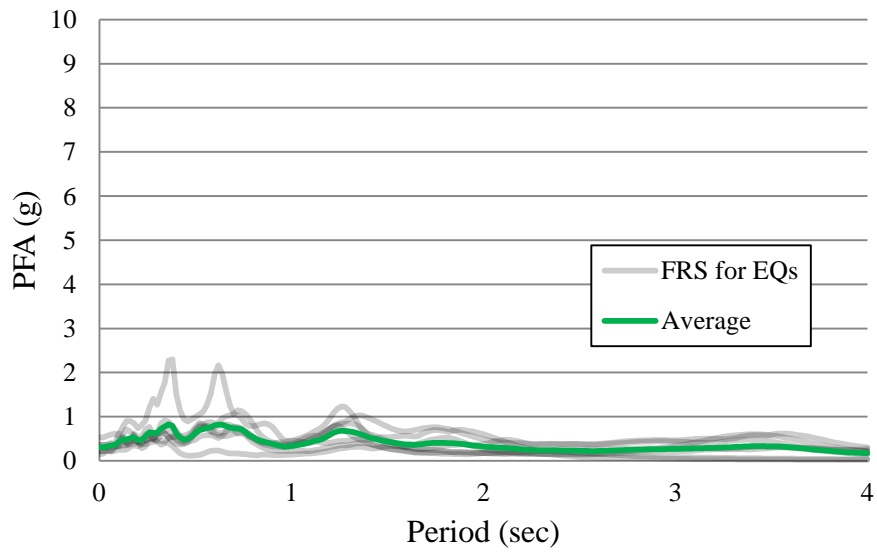
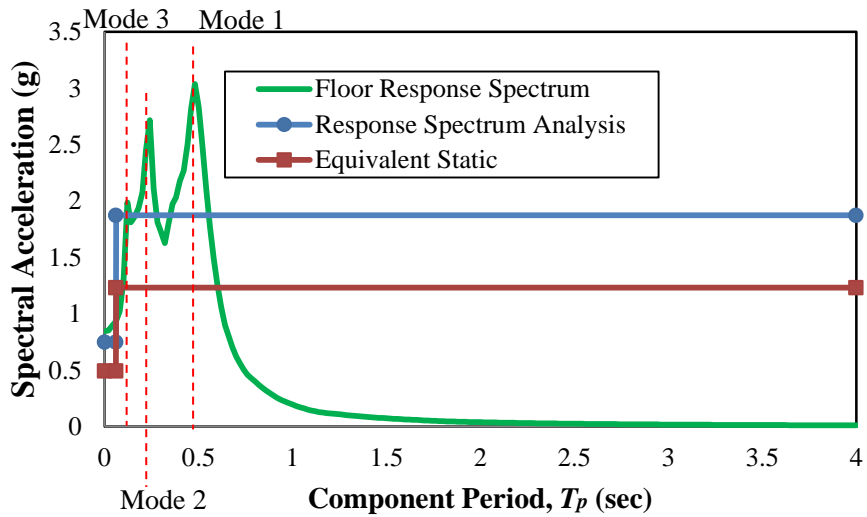
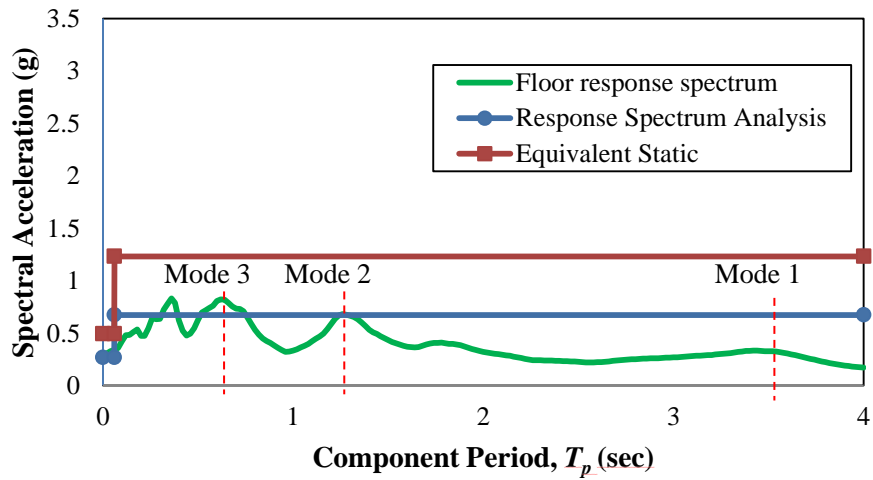


Figure 4-12. Floor Response Spectrum for 20-story SAC model building



(a) Spectral acceleration demand for NSC located at 4-story irregular torsion building



(b) Spectral acceleration demand for NSC located at 20-story SAC model building

Figure 4-13. Floor response spectrum for irregular torsion building and 20-story SAC model building

Figure 4-13 summarizes the results obtained from each building. Figure 4-13(a) is the case of 4-story torsional irregular structure and Figure 4-13 is the case of 20-story regular SAC model that minimized torsional effect. The result shows that the floor response of a building is significantly influenced by the ratio between the period of non-structural component and the fundamental period of building. In case of 20-story SAC model building, the floor response spectrum obviously indicates compelling influence of higher mode effect. Furthermore, the highest response observed when the non-structural component was tuned to the first mode of the 4-story irregular torsion building and second and third mode of the 20-story SAC model regular building. Also, the amplification of component acceleration that has fundamental period close to the fundamental period of the building are typically higher for relatively low rise building and high torsional building as shown in Figure 4-13. The major difference between two buildings is that the irregular torsion building has closely spaced modes of vibration more than the 20-story regular SAC model that results in making the range of tuning effects wider.

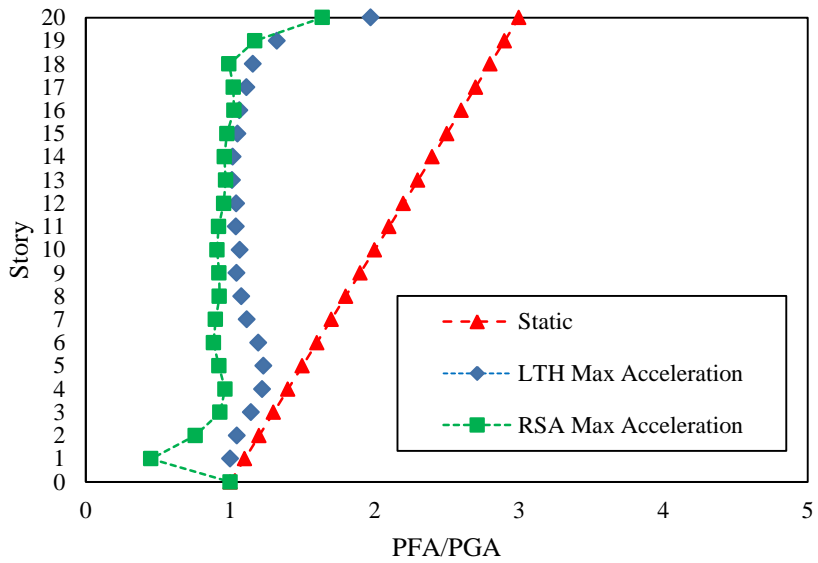


Figure 4-14. Max acceleration demand for NSC located at 20-story SAC model building

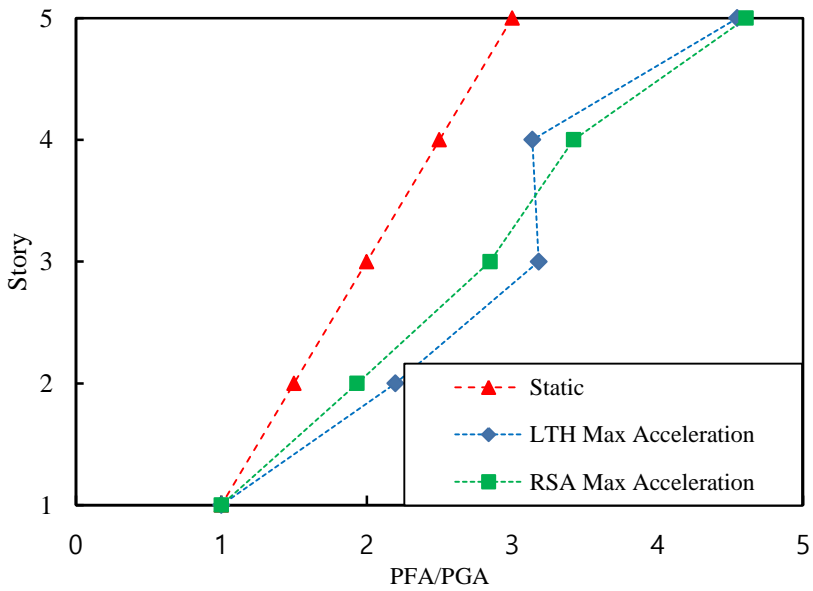


Figure 4-15. Max acceleration demand for NSC located at irregular torsion building

Based on floor response spectrums, maximum acceleration demands for non-structural component were calculated in Figure 4-14 and Figure 4-15. In Figure 4-14 and Figure 4-15, it is shown that estimated response from response spectrum analysis method is very similar to the response from linear time history analysis result. However, there is a major difference between response spectrum analysis method and floor response spectrum. The result from response spectrum analysis considers the interaction between structure and non-structural elements by using dynamic analysis procedure by using equation(2.7). On the other hand, floor response spectrum does not follow typical dynamic analysis procedure since the acceleration demand is directly read from analysis result. Therefore, at present, there is no clear understanding of how interaction between non-structural elements and building may affect a floor response spectrum.

Chapter 5 Case study: Effect of a_p , and R_p application

Table 5-1. Seismic Coefficients for Mechanical and Electrical Components

MECHANICAL AND ELECTRICAL COMPONENTS	a_p	R_p
Air-side HVACR, fans, air handlers, air conditioning units, cabinet heaters, air distribution boxes, and other mechanical components constructed of sheet metal framing	2.5	6
Wet-side HVACR, boilers, furnaces, atmospheric tanks and bins, chillers, water heaters, heat exchangers, evaporators, air separators, manufacturing or process equipment, and other mechanical components constructed of high-deformability materials	1	2.5
Air coolers (fin fans), air-cooled heat exchangers, condensing units, dry coolers, remote radiators and other mechanical components elevated on integral structural steel or sheet metal supports	2.5	3
Engines, turbines, pumps, compressors, and pressure vessels not supported on skirts	1	2.5
Skirt-supported pressure vessels	2.5	2.5
Elevator and escalator components	1	2.5
Generators, batteries, inverters, motors, transformers, and other electrical components constructed of high-deformability materials	1	2.5
Motor control centers, panel boards, switch gear, instrumentation cabinets, and other components constructed of sheet metal framing	2.5	6
Communication equipment, computers, instrumentation, and controls	1	2.5
Roof-mounted stacks, cooling and electrical towers laterally braced below their center of mass	2.5	3
Roof-mounted stacks, cooling and electrical towers laterally braced above their center of mass	1	2.5
Lighting Fixtures	1	1.5
Other mechanical or electrical components	1	1.5

5.1. Acceleration sensitive non-structural component

One of the main purposes of evaluating floor acceleration is to design non-structural component. To include non-structural characteristic to floor acceleration, a_p and R_p value should be considered. As shown in both static and dynamic equation in ASCE7, component amplification factor and component response modification factor will significantly influence the response value because a_p factor varies from 1.00 to 2.50 and R_p factor varies from 1.00 to 12. Several examples are shown in Figure 4-1. Two building

models, one regular and one irregular building, were practiced to evaluate the peak floor acceleration. And then, peak component acceleration has been calculated by using frequently used coefficients for rigid and flexible components. $a_p=1.0$ and $R_p=2.5$ used for case study of rigid components and $a_p=2.5$ and $R_p=3.0, 6.0$ were used for case study of flexible components. Each peak component acceleration was normalized by peak ground acceleration value to estimate the amplification along the height of the building.

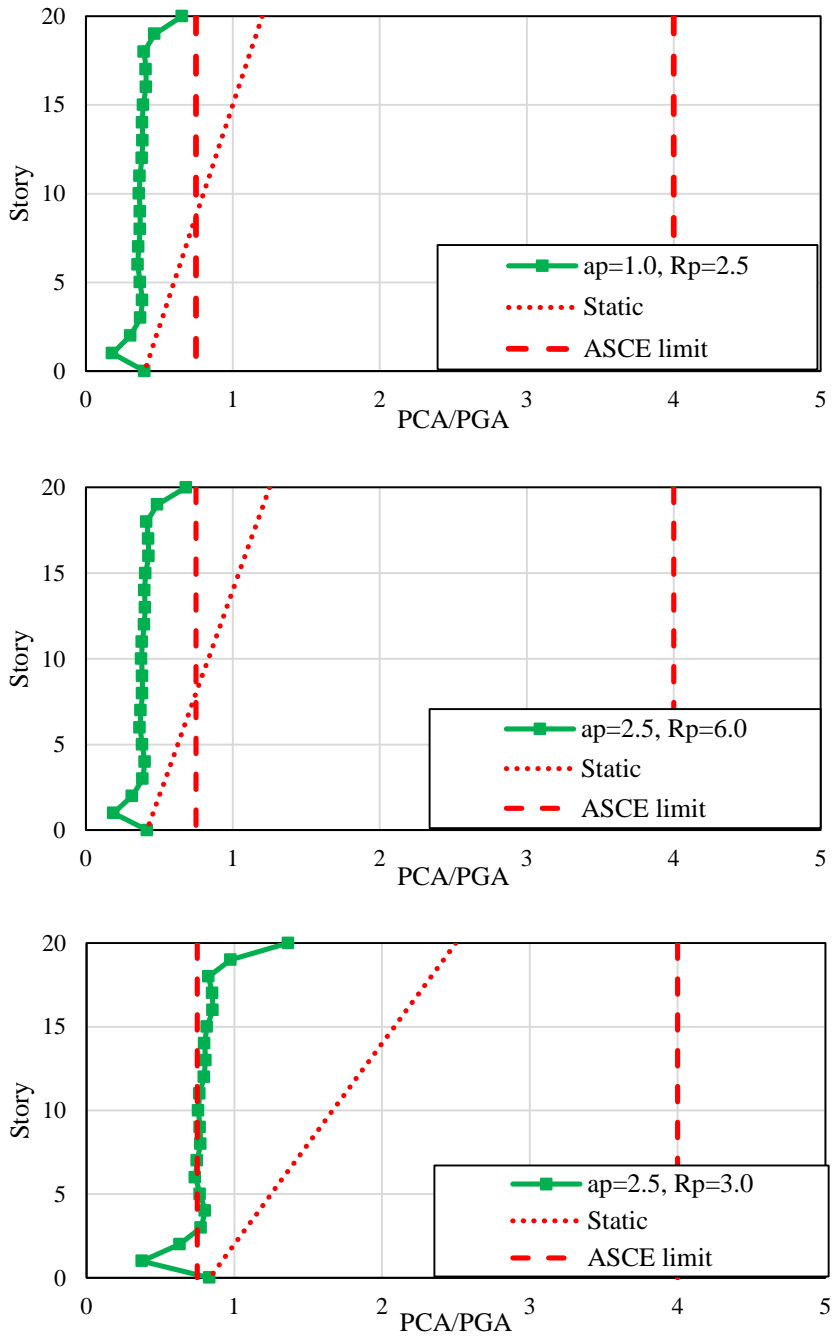


Figure 5-1. Amplification of peak component acceleration of 20-story regular building

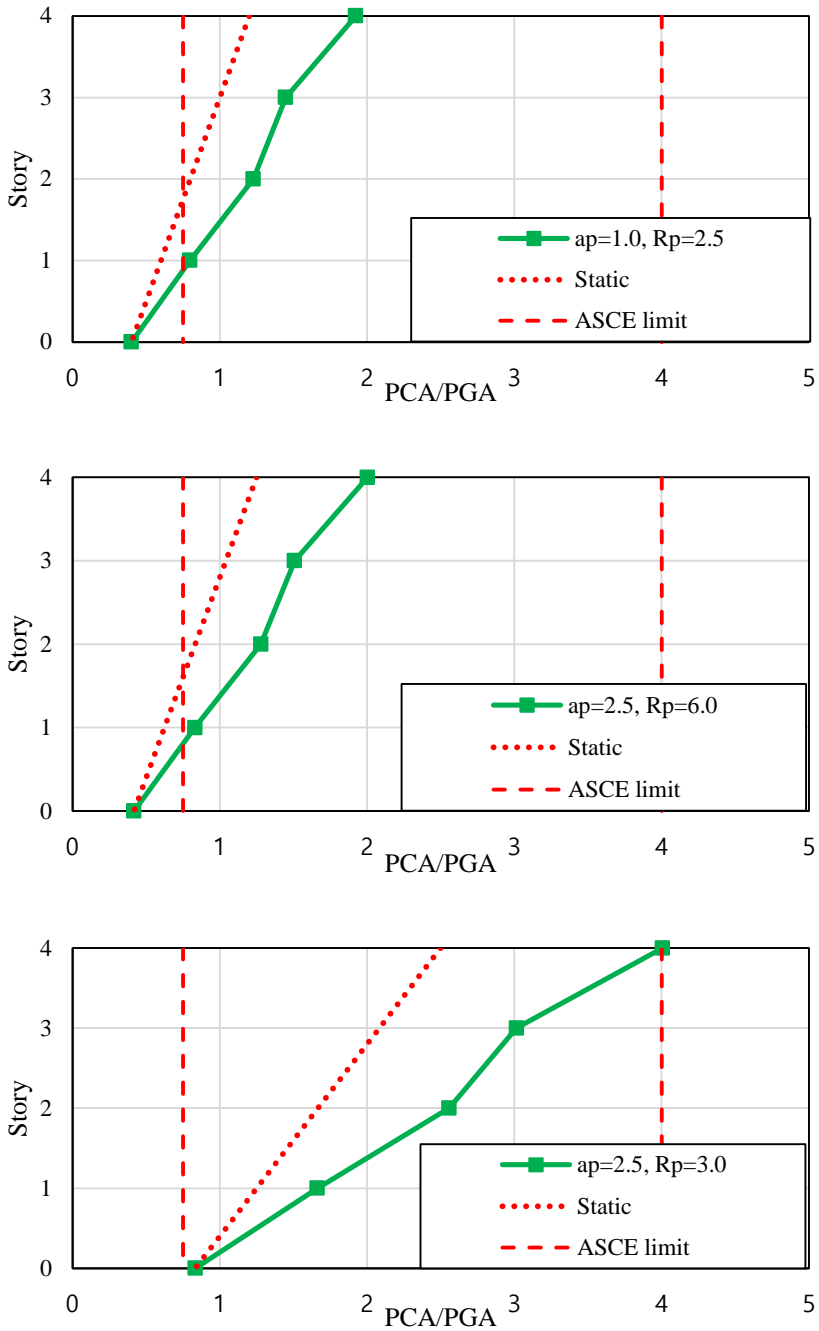


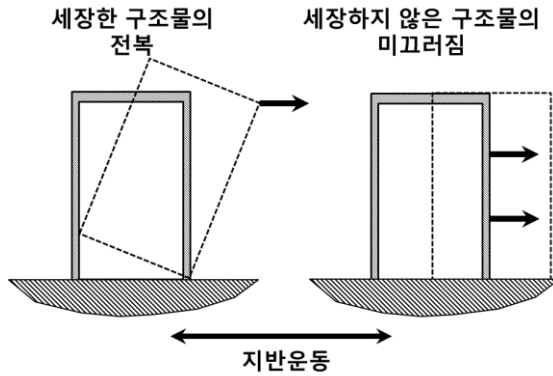
Figure 5-2. Amplification of peak component acceleration of 4-story irregular building

Figure 5-1 evaluates the peak component acceleration applied to non-structural elements in 20-story SAC model regular building. Non-structural characteristic was reflected by non-structural coefficients mentioned above. Frequently used values for both flexible and rigid components were selected from ASCE7 chart. In Figure 5-1, the result obviously shows that both static and dynamic amplification were reduced since R_p value is higher than a_p value. However, the upper and lower limits from ASCE7 does not change because a_p and R_p values only depends on short period spectral acceleration (S_{DS}), and component importance factor (I_p). Therefore, in case of 20-story regular building, lower limit of ASCE governs the floor response to design non-structural components.

Figure 5-2 demonstrates the behavior of 4-story irregular torsion building. The result also shows that seismic coefficients significantly decrease both static and dynamic result but the upper and lower bound stays same. Flexible non-structural components that have high R_p value shows similar acceleration demand with rigid component. However in case of irregular torsion building, dynamic analysis gives more conservative result than static result of irregular torsion building. In case when a_p value is close to R_p value, the roof level response is higher than static response, which is still governed by upper bound.

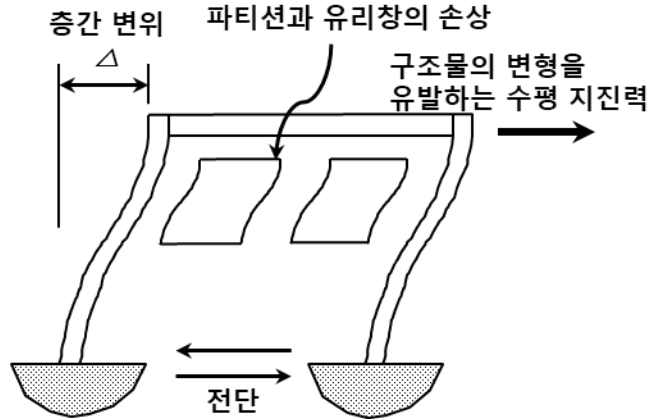
5.2. Deformation sensitive non-structural component

The failure modes of acceleration sensitive non-structural components depends heavily on higher mode effect, nonlinearity, torsion and floor response spectrum, which are normally overturning, and sliding(Figure 5-3(a)). Water tank, telecommunication equipment rack or air conditioner



(a) Damage due to inertial forces

(Acceleration sensitive non-structural component)



(b) Damage due to excessive deformation

(Deformation sensitive non-structural component)

Figure 5-3. Typical behavior of non-structural component(FEMA E-74, 2011)
 are examples of acceleration sensitive non-structural elements. Even though only the acceleration sensitive non-structural elements were considered through this thesis, many of the other non-structural components are deformation sensitive such as curtain wall, partition, veneer, and masonry walls. The behavior of deformation sensitive non-structural component is caused by excessive deformation as shown in Figure 5-3.

Table 5-2. Response sensitivity classification of non-structural component (FEMA 274, 1997)

Component	Sensitivity		Component	Sensitivity		
	Acc.	Def.		Acc.	Def.	
Architectural			Mechanical Equipment			
1	Exterior skin		1	Mechanical Equipments		
	Adhered Veneer	S P		Boilers and Furnaces	P	
	Anchored Veneer	S P		General Mfg. and Process Machinery	P	
	Glass Blocks	S P		HVAC Equipment, Vibration Isolated	P	
	Prefabricated Panels	S P		HVAC Equipment, Nonvibration Isolated	P	
	Glazing Systems	S P		HVAC Equipment, Mounted In-line with Ductwork	P	
2	Partitions		2	Storage Vessels and Water Heaters		
	Heavy	S P		Structurally Supported Vessels	P	
	Light	S P		Flat Bottom Vessels	P	
3	Interior Veneers		3	Pressure Piping		
	Stone, Including Marble	S P	4	Fire Suppression Piping		
	Ceramic Tile	S P	5	Fluid Piping, not Fire Suppression		
Ceilings		Hazardous Materials		P	S	
Directly Applied to Structure	P	Nonhazardous Materials		P	S	
4	Dropped, Furred Gypsum Board	P	6	Ductwork		
	Suspended Lath and Plaster	S P		P	S	
	Suspended Integrated Ceiling	S P				
5	Parapets and Appendages					
6	Canopies and Marquees					
7	Chimneys and Stacks					
8	Stairs					

Acc. = Acceleration Sensitive / Def. = Deformation sensitive
P = Primary Response / S = Secondary Response

According to Table 5-2, it is shown that most of mechanical and electrical equipment is generally acceleration sensitive since most equipment is usually anchored or attached to the ground; therefore, failure modes of non-structural elements are composed of sliding, overturning or tilting of items mounted on the floor or roof. On the other hand, the major part of architectural non-structural components are deformation sensitive components that are typically used as a wall structures such as veneer, glass blocks, panels,

partitions. However, elevated architectural structures such as suspended ceilings chimneys or stairs are considered as acceleration sensitive structures.

For deformation sensitive non-structural components, there are drift limits suggested by Gillengerten (2001) is shown below:

Table 5-3. Drift limits for deformation sensitive components (Gillengerten, 2001, 681-721)

Component	Performance Objective	
	Life Safety	Immediate Occupancy
Adhered Veneer	0.03	0.01
Anchored Veneer	0.02	0.01
Nonstructural Masonry	0.02	0.01
Prefabricated Wall Panels	0.02	0.01
Glazing Systems	0.02	0.01
Heavy Partitions	0.01	0.005
Light Partitions	Not required	0.01
Interior Veneers	0.02	0.01

Table 5-3 shows that the drift limits expected to generate severe damage to the non-structural components at the life safety level, moderate damage to the immediate occupancy level. Drift limits are considered accounts to the flexible couplings, sliding joints or deformation of ductile elements in the component or system.

Chapter 6 Summary and Conclusions

In this thesis, the equivalent static analysis was evaluated by theoretical and numerical analysis including several key parameters that might influence the maximum floor acceleration. Several dynamic analyses were performed and analyzed to clarify the effect of key influential parameters such as torsion, higher mode effect, nonlinearity and floor response spectrum.

Theoretical analysis and numerical analysis showed that the maximum floor acceleration should be based on the structural period-dependent spectral acceleration (S_a) instead of S_{DS} which is not affected by structural period. The floor acceleration demand calculated based on the equivalent static approach is expected to be conservative for high-rise buildings with long period due to the higher mode effect. Also, the assumption of linear distribution along the building height could be significantly violated due to the higher mode effect.

Nonlinearity of the supporting structure significantly reduced the peak floor acceleration because the floor acceleration gets lower when frames undergo yielding process. However, the actual acceleration that non-structural component would experience may vary depending on the tuning ratio when the structure starts to yield.

For irregular torsion buildings, the torsional amplification factor was as high as 2.7, which implies the essential consideration of torsional effect during the design process. In ASCE 7-16, the equivalent static approach does not consider torsional effect while the dynamic analysis result is critically

influenced by torsion and draws much higher output as shown in this thesis. This seems technically unfair; therefore, the inclusion of applicable torsional amplification to the equivalent static approach appears necessary.

Numerical analysis result of torsion building reveals possibilities of developing accuracy of torsional amplification factor since the analysis draws conservative result. The value at the joint farthest from the center of rigidity, the maximum floor acceleration from structural analysis, is recommended to be used regardless of the torsional irregularity. However, there are some remaining engineering judgements for floor acceleration that should be adapted to design non-structural elements on the floor as mentioned in this thesis.

Floor response spectrum result indicates that the response on non-structural element is strongly dependent on the fundamental modal periods and the types of lateral-load resisting system. To use floor response spectrum method, it is necessary to consider mass ratio and tuning effect for more rational seismic design of non-structural elements.

The case study of 20-story regular building and 4-story irregular torsional building shows that applying non-structural characteristics, a_p and R_p values, to estimate floor spectrum significantly changes the acceleration demand. In both cases, static and dynamic result reduces when a_p and R_p values applied but lower and upper bound stays same since limits does not include non-structural aspect. Therefore, lower limit governs the response of 20-story regular building for frequently used non-structural properties. On the other hand, in case of 4-story irregular torsional building, although the

response of both static and dynamic result has been decrease, the response is still higher than static result. The roof level response of irregular building is still high enough to be governed by ASCE upper limit.

Based on numerical study and theoretical study, key influential structural parameters such as fundamental period, higher modes, nonlinearity and torsion should be selectively included to the current static analysis method considering practicality.

Bibliography

- [1] Anajafi, H., Medina, R.A. (2018a). “Effects of supporting building characteristics on non-structural components acceleration demands,” *Eleventh U.S. National Conference on Earthquake Engineering*, California, USA.
- [2] Anajafi H., Medina R.A. (2018b) “Evaluation of ASCE 7 equations for designing acceleration-sensitive nonstructural components using data from instrumented buildings,” *Earthq Eng Struct Dyn*, Vol. 47, No. 4, 1075–1094.
- [3] ASCE/SEI, 7-16 (2017). *Minimum design loads and associated criteria for buildings and other structures*. American Society of Civil Engineers, Reston, VA, USA.
- [4] ASCE/SEI, 41-13 (2013). *Seismic evaluation and retrofit of existing buildings*. American Society of Civil Engineers, Reston, VA, USA.
- [5] Chopra, Anil K. *Dynamics of Structure: Theory and Applications to Earthquake Engineering*. 3rd ed., Pearson/Prentice Hall, 2007.
- [6] Drake RM, Bachman RE. (1995). “Interpretation of instrumented building seismic data and implications for building codes,” *Proceedings of the 64th Annual Convention, Structural Engineers Association of California, Structural Engineers Association of California*; pp. 333–344, October, California, USA.
- [7] CEN, European Committee for Standardization. (2004). EN 1998-1, *Eurocode 8: Design of structure for earthquake resistance, Part 1.1:*

- General rules, seismic actions and rules for buildings*. Brussels: BSi
- [8] Gillengerten, J. D. (2001). Design of Nonstructural Systems and Components. In F. Naeim (Ed.), *The Seismic Design Handbook* (pp. 681-721). Boston, MA: Springer US.
- [9] Gupta, A., Krawinkler, H. (1999). "Seismic demands for performance evaluation of steel moment resisting frame structures," *Report No. 132*, Department of Civil and Environmental Engineering, Stanford University, USA.
- [10] Kehoe, B.E., Freeman, S.A. (1998). "A critique of procedures for calculating seismic design forces for non-structural elements," *Applied Technology Council-29-1*, California, USA.
- [11] Lee, Cheol Ho, et al. "Evaluation of Equivalent Static Analysis Method for Seismic Design of Non-Structural Elements." *SPONSE (International Association for the Seismic Performance of Non-Structural Elements)*, vol. 4th, 22 May 2019.
- [12] *National Earthquake Hazards Reduction Program (NEHRP) Reauthorization: Hearing before the Subcommittee on Science, Technology, and Space of the Committee on Commerce, Science, and Transportation, United States Senate, One Hundred Third Congress, Second Session, May 17, 1994*. U.S. G.P.O., 1994.
- [13] Seismology Committee. (1988). Recommended lateral force requirements and commentary, SEAOC, Sacramento, CA, USA.
- [14] Singh, M., Suarez, L. (1987). "Seismic response analysis of structure–equipment systems with non-classical damping effects," *Earthquake*

- Engineering & Structural Dynamics*, Vol. 15, No. 7, pp.871-888.
- [15] Building Seismic Safety Council. (1997). *NEHRP commentary on the guidelines for the seismic rehabilitation of buildings*. Washington, D.C.: Department of Homeland Security.
- [16] Applied Technology Council. (2011). *Reducing the risks of nonstructural earthquake damage: A practical guide*. Redwood City, CA: U.S. Department of Homeland Security.
- [17] Villaverde, R. (2000). Design-oriented approach for seismic nonlinear analysis of nonstructural components. In *Proceedings of the 12th World Conference on Earthquake Engineering, Paper* (No. 1979).
- [18] Villaverde R. (2004). "Seismic Analysis and Design of Nonstructural Elements." *Earthquake Engineering from engineering seismology to performance-based engineering*. Ed. Yousef Bozorgnia, Ed. Vitelmo V. Bertero. Florida: 2004. 1140-1198. Print.
- [19] *1997 Uniform Building Code*. International Conference of Building Officials, 1997.

Abstract (in Korean)

최근 2 년간 한국에서는 리히터 규모 5.8의 경주지진(2016)과 5.4의 포항지진(2017)이 연달아 발생하며 수많은 재산피해를 입히고 더 이상 한국은 지진의 안전지대가 아니라는 사실과 함께 국민들에게 지진에 대한 경각심을 불러일으켰다. 특히 이번 포항지진에서는 보나 기둥, 슬래브등의 구조요소의 피해뿐만 아니라 비구조요소의 피해규모가 컸기 때문에 비구조요소의 내진설계에 대한 관심이 높아진 것이 사실이다. 건축구조기준에 따르면 건축구조요소뿐만 아니라 구조내력을 부담하지 않는 비구조요소인 비구조벽체, 이중바다, 천장 및 캐비닛 등도 기준을 따라야 한다고 명시되어 있지만 사실상 적용사실유무는 확인하기 어려운 실정이다.

이번 연구에서는 비구조요소의 내진설계를 위해 일반적으로 사용되는 방법인 등가 정적해석법을 평가하여 현행 코드를 발전시킬 수 있는 가능성을 모색하였다. 현재 설계코드를 평가하기 위해 ASCE7를 검토해 현행 코드 조항에 제시되어 있는 등가정적 접근방식의 문제점을 분석한다. 건물의 고유주기를 고려한 동적해석법을 사용해 등가정적해석법의 문제점을 밝혀내고 구조해석 프로그램을 사용하여 수치해석적 결과를 분석하였다. ASCE7-16의 선형 정적해석과 동적해석을 기반으로 층응답 분석을 수행하였으며 수치해석은 총 5개의 3차원 건물모델들을 평가하였고 첫 번째 파트에서는 3층, 9층, 20층의 3차원 SAC건물 모델을 평가하였고 두 번째 파트에서는 비정형성이 있는 4층, 8층 통신건물을 분석하였다.

동적분석은 응답 스펙트럼 해석, 선형 시간이력 해석, 비선형 시간이력 해석 및 간략 층응답 스펙트럼 해석을 포함하는데 이번 연구에서는 응답 스펙트럼 해석, 선형 시간이력 해석과 비선형 시간이력 해석을 수행하였다. 등가정적해석과 동적해석의 결과는 주로 비구조요소를 위한 층응답스펙트럼을 구하기 위해 사용되는데

이는 각 층의 최대 가속도가 지진의 영향을 받고있는 비구조요소의 내진설계 과정을 단순화 시켜주기 때문이다. 일반적으로 스펙트럼 분석에 대한 평가는 2차원 수치해석 모델에 크게 의존하기 때문에 중요한 매개변수들을 고려하기 위해서는 3차원 모델의 수치해석이 필요하다.

따라서 본 연구에서는 현실적인 3차원 수치해석 모델의 기초 구조역학과 수치해석 연구를 바탕으로 등가정적해석법을 평가하였다. 기초 구조역학을 통해 건물의 고유주기를 반영하지 않은 등가정적해석법이 정확하지 않다는 것이 명확하게 설명된다. 또한 3차원 건물 모델의 동적 수치해석은 최대 층응답의 크기와 분포가 고유주기, 고차모드, 비선형성 및 비틀림과 같은 건물 특성에 따라 크게 영향을 받을 수 있음을 보여준다. 현행 등가 정적 방법은 일부 영향력 있는 매개변수가 실용성을 고려한 한계 내에서 선택적으로 포함되도록 개선될 필요가 있다.

주요어: 비구조요소, 층가속도, 등가정적하중, 비틀림, 고차모드영향, 비선형성

학번: 2017-28610